CHEMISTRY
A EUROPEAN JOURNAL

DOI: 10.1002/chem.200902551

Preparation of "Si-Centered" Chiral Silanes by Direct α-Lithiation of Methylsilanes

Christian Däschlein, Viktoria H. Gessner, and Carsten Strohmann*[a]

Abstract: The direct α-lithiation of methyl-substituted silanes as an efficient method for the preparation and elaboration of Si-chiral compounds is reported. Deprotonation of chiral oligosilanes occurs selectively and with high yields at the methyl group of the stereogenic silicon center, even in the presence of multiple methylsilyl or methylgermyl substituents. Computational studies have confirmed this preference as a consequence of pre-coordination of the lithiating agent by the amino side-arm and repulsion effects in the corresponding transition state. This complexation is also obvious from X-ray structure analyses of the α-lithiated silanes, which exhibit intriguing structure formation patterns differing in the type of aggregation and the amount of alkyllithium used. An alternative route to Si-chiral compounds is also presented, which involves desymmetrization of dimethylsilanes mediated by a chiral side-arm. Structure analyses and computational studies have shown that the diastereoselectivity of this α-lithiation is influenced by the selectivity of the formation of the stereogenic nitrogen upon complexation of the alkyllithium.

Keywords: chirality · lithium · organolithium compounds · organosilicon · structure elucidation

Introduction

Functionalized silicon compounds are well known for their applications in various fields of chemistry, for example as protecting or activating groups in organic synthesis.[1] In recent years, the use of chiral silicon systems has become of particular interest due to their application as auxiliaries in stereoselective synthesis.[2] In this context, silicon groups with a stereogenic silicon center have attracted a great deal of attention owing to the high selectivities that can be achieved in a variety of reactions, such as silicon-to-element (especially carbon and silicon) chirality transfers,[3] Mannich reactions,[4] cycloaddition reactions,[5] Friedel–Crafts alkylations,[6] and aldol reactions,[7] as well as in the kinetic resolution of chiral secondary alcohols.[8] Despite this high synthetic potential of silicon-chiral silanes in preparative chemistry, many of their properties and applications are as yet not fully understood or even remain unexplored due to the extremely limited number of suitable preparation methods.

Silanes with a stereogenic silicon center are accessible through three general methodologies.

i) The first method is the separation of stereoisomers by the formation of diastereomers.[9] These diastereomeric silanes can then be separated by standard resolution methods, principally chromatography and crystallization. In the case of crystallization, there have been examples of target silanes that already possessed two or more stereocenters (diastereomers) and thus did not require any additional reaction step for their separation.[10] For compounds with only one stereocenter (enantiomers), the formation of diastereomers by the addition of a chiral auxiliary has proved to be the method of choice. One recent example is the treatment of aminomethyl-functionalized silanes with mandelic acid,[11] which resulted in quaternization of the nitrogen in the side-arm of the molecule to form diastereomeric salts with different crystallization properties. However, although this method has generally proved to be highly efficient, it is severely limited as only a few systems with suitable crystallization behavior have as yet been identified.

ii) The second methodology for the synthesis of Si-centered chiral silanes is the transformation of stereochemically pure compounds to new chiral molecules. In particular,

[a] Dr. C. Däschlein, Dr. V. H. Gessner, Prof. Dr. C. Strohmann
Anorganische Chemie, Technische Universität Dortmund
Otto-Hahn-Strasse 6, 44227 Dortmund (Germany)
Fax: (+49) 231-755-7063
E-mail: mail@carsten-strohmann.de

Supporting information for this article is available on the WWW under http://dx.doi.org/10.1002/chem.200902551: Crystallographic data of the presented compounds and aggregates; full computational details.

the cleavage of silicon–silicon or silicon–carbon bonds with elemental lithium, thereby forming enantiomerically pure lithiosilanes, has been used for their preparation.[11–13] Subsequent trapping of the lithiated species with electrophiles such as chlorosilanes or alkyl halides results in the formation of novel stereochemically pure silicon-chiral compounds. However, the lithiosilanes involved can potentially lose stereo-information during the reaction process due to their relatively low configurative stabilities.[14] Although they are significantly more stable than the corresponding carbon compounds, selective transformations to stereochemically pure trapping products can only be accomplished at low temperatures (−30 °C and lower) at which racemization is inhibited.

iii) Recently, some initial reports have appeared concerning the use of chiral auxiliaries such as (*R*)-BINAP or (*R*,*S*)-JOSIPHOS for the synthesis of silicon-chiral silanes. The treatment of achiral reactants with metal salts and the chiral ligand results in the formation of enantiomerically enriched silanes. However, the generality of application of this method is still less than adequate and thus the potential of the reaction is as yet extremely limited.[15] Scheme 1 summarizes the three described methods for the preparation of enantiomerically enriched and pure Si-chiral silanes.

As part of our studies on stereochemically enriched and pure silanes, we present herein the synthesis of Si-chiral compounds by direct α-lithiation of methyl groups at silicon. Two different synthetic routes are presented, namely the selective transformation of an already stereochemically pure Si-chiral species to a new chiral molecule and the diastereoselective α-lithiation of a dimethylsilane via a chiral sidearm. The potential of this method is underlined by the accomplishment of a variety of trapping reactions. The stereochemical course of the presented deprotonation reactions has been proved by X-ray diffraction analyses of the lithiated intermediates. Further structural analyses in combination with computational examinations have provided insight into the reaction mechanism and the observed selectivities.

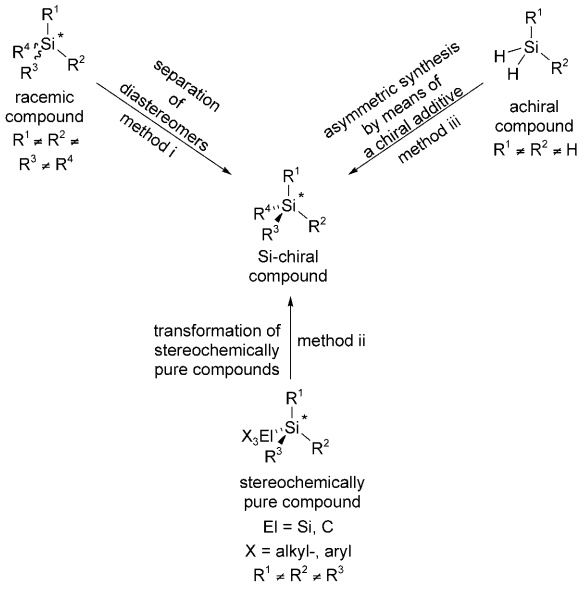

Scheme 1. Common methodologies for the preparation of silicon-chiral silanes.

Results and Discussion

In recent years, our group has reported several synthetic pathways to enantiomerically pure tri- and tetrasilanes, as well as silagermanes, based on trapping reactions of enantiomerically pure lithiosilanes with chlorosilanes and chlorogermanes (see Figure 1 for selected examples).[11,12a,b]

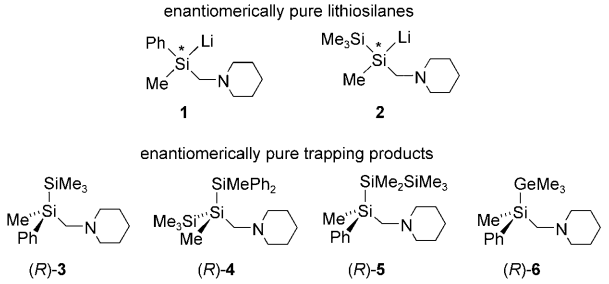

Figure 1. Selected examples of highly enantiomerically enriched di- and trisilanes as well as one silagermane that could be synthesized via enantiomerically pure lithiosilanes.

However, due to the lack of configurative stability of the intermediate lithiosilanes, further variants for direct transformations of the enantiomerically enriched silanes without a labile intermediate are highly desired. The best method would be a direct functionalization of the substituents bonded to the silicon without the involvement of the central, stereogenic silicon atom. As all hitherto reported highly enantiomerically enriched silanes have possessed at least one methyl group at each silicon (or germanium) atom, direct functionalization by deprotonation seemed to be a promising strategy. Although such direct deprotonation of methyl groups at silicon atoms in silanes is in general highly disfavored,[16] so-called "side-arm complexation" of amino-functionalized silanes proved to be the method of choice for enabling this reaction.[17] The general concept for this deprotonation reaction is based on Klumpps' idea[18] of oxygen- and nitrogen-assisted lithiations, and it has recently been used for the synthesis of functionalized α-lithiated silanes with additional stabilizing groups close to the lithiated center (e.g., benzylsilanes).[19] To the best of our knowledge, this reaction has not yet been studied in relation to oligosilanes with a stereogenic silicon center, and in this regard we especially wanted to address two central questions: i) Can a simple methyl group in an oligosilane be directly deprotonated by treatment with alkyllithium bases? ii) If so, can we also accomplish regio- and stereoselective deprotonation re-

actions in molecules with more than one methyl group at the silicon atom?

Synthesis of α-functionalized, enantiomerically pure silanes by selective α-lithiation of enantiomerically pure reactants: The trimethylsilyl-substituted disilane **3** seemed to be particularly suitable for these investigations. This compound possesses four methyl groups that, in principle, might be deprotonated. Furthermore, the steric demand of the whole system is relatively low, and thus the necessary approach of the alkyllithium base to the silane should be possible. To evaluate the potential of the lithiation reaction for the functionalization of such silicon compounds, the racemic silane *rac*-**3** was chosen as a first starting system. Thus, a solution of *rac*-**3** in *n*-pentane was treated with one equivalent of *tert*-butyllithium for 5 h at room temperature. *t*BuLi was chosen as it is the strongest commonly used alkyllithium base. Trimethylchlorostannane was subsequently added to the reaction mixture at −78 °C. To examine the reaction process and the formed compounds, the crude product was analyzed by NMR and GC/MS. Only one α-stannyl-functionalized silane could be identified. The treatment of **3** with *tert*-butyllithium had resulted in selective deprotonation of the methyl group at the stereogenic silicon center, even though there are four possible reactive methyl groups in the molecule. The formed α-stannyl-functionalized silane *rac*-**8** could be isolated after work-up in an overall yield of 77% (see Scheme 2). Likewise, the analogous trapping reaction of the α-lithiated silane with paraformaldehyde as electrophile resulted in the formation of the β-hydroxysilane *rac*-**9** in 85% yield.

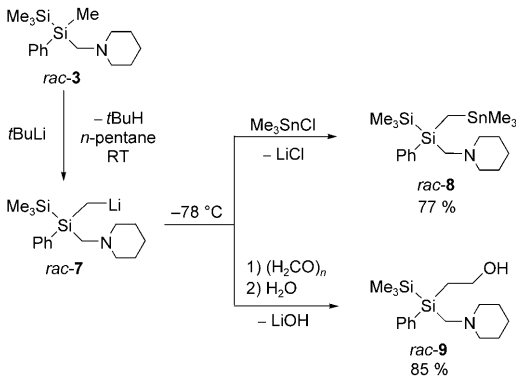

Scheme 2. Synthesis of the racemic, α-functionalized silanes *rac*-**8** and *rac*-**9**.

Following the successful application of direct lithiation to the racemic compound, the enantiomerically pure disilane (*R*)-**3** was subjected to the whole reaction sequence to examine the feasibility of this method for the preparation of α-functionalized enantiomerically pure silanes. The same regioselectivity was observed in the α-lithiation of (*R*)-**3**, with exclusive deprotonation of the methyl group at the stereogenic silicon center (see Scheme 3). Detailed NMR studies revealed the formation of both trapping products, (*R*)-**8**[20] and (*R*)-**9**,[21] under full preservation of the stereo-information of the chiral silicon center with e.r. values >99:1. Thus, the following two results may be noted: 1) Treatment of the disilane **3** with *tert*-butyllithium results in selective deprotonation of the methyl group at the stereogenic silicon center, and this may be exploited for selective functionalization. 2) As the stereogenic silicon center is not involved in the reaction, enantiomerically pure, functionalized silanes are easily accessible.

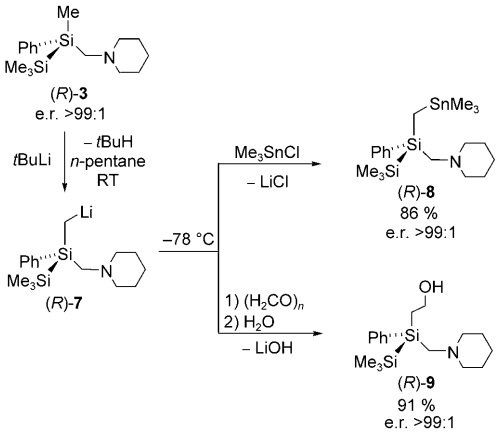

Scheme 3. Synthesis of the enantiomerically pure, α-functionalized silanes (*R*)-**8** and (*R*)-**9**.

Based on these promising results pertaining to the selective deprotonation of the disilane (*R*)-**3**, we sought to expand the method to the related trimethylgermyl-substituted silagermane (*R*)-**6**. Therefore, a solution of (*R*)-**6** in *n*-pentane was treated with one equivalent of *tert*-butyllithium for 5 h at room temperature and the intermediate was subsequently trapped with trimethylchlorostannane at −78 °C. NMR and GC/MS analyses of the crude product confirmed that selective deprotonation of the methyl group at the stereogenic silicon center had also occurred in the silagermane (*R*)-**6**. After work-up, the α-stannyl-functionalized silagermane (*R*)-**11** was isolated in an overall yield of 95% (see Scheme 4).

Analogous reactions were performed with the trisilane *rac*-**4**. However, we changed the trapping reagents from paraformaldehyde and trimethylchlorostannane to deuterium oxide and dimethyldichlorogermane to broaden the range of trapping reagents used. As the main focus of this reaction concerned the divergent trapping reagents, it was only carried out using the racemic compound *rac*-**4**, which is more

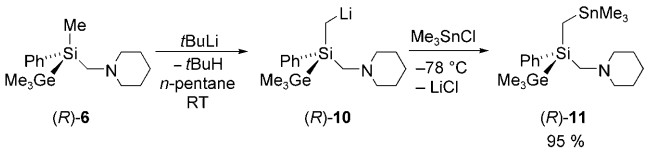

Scheme 4. Synthesis of the enantiomerically pure, α-functionalized silagermane (*R*)-**11**.

easily accessible. Nevertheless, we postulate the same reactivity for the enantiomerically pure trisilane. Compared to the disilane **3**, the phenyl group is substituted by the significantly more sterically demanding diphenylmethylsilyl group. In total, five different methyl groups are present in the molecule, resulting in three different possible reactive centers. This raised the question as to whether the regioselective deprotonation would still be possible despite the steric congestion of the system. Therefore, after stirring with *t*BuLi for 5 h, the intermediate was trapped with either D_2O or Me_2GeCl_2. In both cases, NMR and GC/MS analyses of the crude product confirmed selective deprotonation of the trisilane at exclusively one position (see Scheme 5), the methyl group at the stereogenic silicon center.

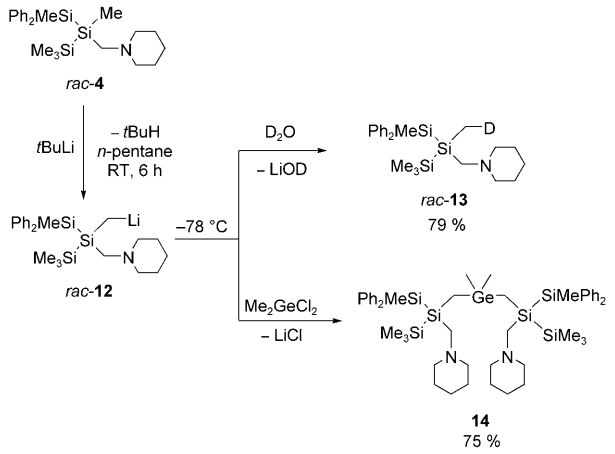

Scheme 5. Synthesis of the enantiomerically pure, α-functionalized silanes *rac*-**13** and **14**.

Overall, these lithiation reactions prove that the treatment of aminomethyl-functionalized oligosilanes with *t*BuLi is a facile and useful method for the regioselective deprotonation of the methyl group at the stereogenic silicon center and thus for the elaboration of enantiomerically pure, α-functionalized systems.

Structural studies: To obtain a profound and detailed insight into the reaction process, the lithiated intermediates were crystallized and their structures were determined by X-ray diffraction analysis. To this end, one equivalent of each oligosilane was treated with one equivalent of *tert*-butyllithium, and the mixture was stirred for 5 h at room temperature and then stored at −78 °C (−30 °C in the case of the lithiation of trisilane **4**). In this way, single crystals of the lithiated disilane (*rac*-**7**)$_4$ as well as of the lithiated trisilane (*rac*-**12**)$_2$ could be isolated. In addition, all compounds were analogously treated with two equivalents of *t*BuLi, which yielded the different crystalline solids [(*R*)-**7**·(*t*BuLi)]$_2$ and [(*R*)-**10**·(*t*BuLi)]$_2$. Interestingly, three different types of molecular structures could be identified in the X-ray diffraction analyses.

The lithiated disilane (*rac*-**7**)$_4$ crystallized from *n*-pentane in the tetragonal crystal system with space group $P42_1/c$ as a tetrameric structure with a central lithium tetrahedron with an average side length (Li–Li distance) of 2.72(8) Å (see Figure 2). As is typical for such tetrameric alkyllithiums, the Li_3 triangles are μ_3-capped by the carbanionic centers, resulting in three contacts between each deprotonated carbon atom and the lithium atoms.[22] The Li–C distances are between 2.249(5) and 2.416(5) Å, and are thus in the typical range for oligomeric alkyllithium compounds, as exemplified by (*t*BuLi)$_4$.[22] The lithium atoms are coordinated by the aminomethyl side-arm of the disilane unit, which stabilizes the whole system by completing the coordination sphere of the lithium.

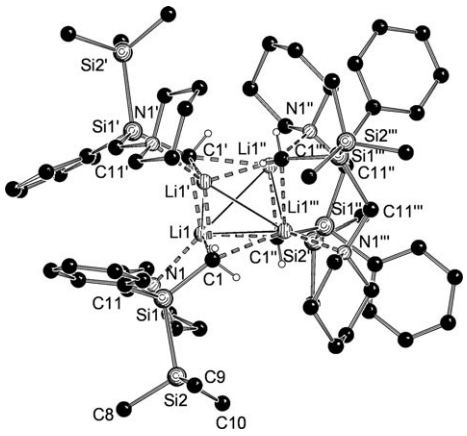

Figure 2. Molecular structure of the lithiated silane (*rac*-**7**)$_4$ in the crystal. All hydrogen atoms except those on the lithiated carbon centers, as well as the numbering scheme of the hydrogen atoms and most of the carbon atoms, have been omitted for clarity. Selected bond lengths [Å] and angles [°]: C1–Si1 1.844(3), C2–Si1 1.898(3), C1–Li 2.249(5), C1–Li′ 2.301(5), C1–Li″ 2.416(5), C11–N1 1.479(4), C11–Si1 1.906(3), Li–N1 2.160(5), Li–C1′ 2.301(5), Li–C1‴ 2.416(5), Li–Li′ 2.466(9), Li–Li″ 2.849(8), Li–Li‴ 2.849(8), Li–Si1 3.103(5), Si1–Si2 2.3677(11); Si1-C1-Li 98.12(17), N1-Li-C1 97.8(2); symmetry operations to generate equivalent atoms: ′: $-x+1, -y+1, z$; ″: $y, -x+1, -z+2$; ‴: $-y+1, x, -z+2$.

Surprisingly, treatment of (*R*)-**3** with two equivalents of *t*BuLi also resulted in the formation of a tetrameric structure, albeit with a different composition. In this case, a mixed aggregate of *t*BuLi and the lithiated disilane was formed, in which the central Li_4 tetrahedron consisted of two molecules of the α-lithiated disilane and two molecules of the sterically less bulky *t*BuLi (see Figure 3).[23] [(*R*)-**7**·(*t*BuLi)]$_2$ crystallized from *n*-pentane in the hexagonal crystal system, space group $P6_4$. In this structure, the average side length (Li–Li distance) of the central Li_4 tetrahedron amounts to 2.59(9) Å, which is significantly shorter than that in the structure of the racemic disilane. This bond shortening is due to the decreased spatial demand upon the incorporation of the *t*BuLi units instead of the disilane molecules. Again, the Li–C contacts (2.290(8)–2.299(6) Å) are in the typical range for this class of compounds. Consequently, the use of either one or two equivalents of *t*BuLi results in selective deprotonation of the methyl group at the stereogenic

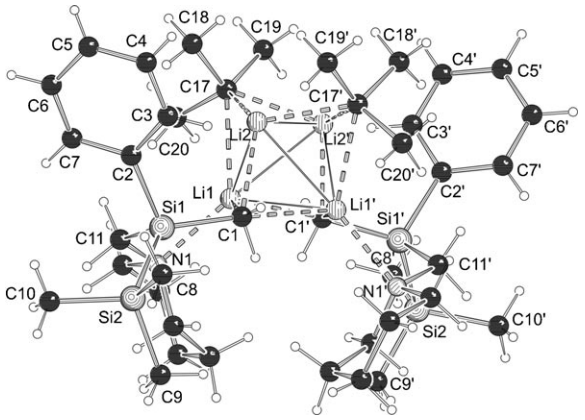

Figure 3. Molecular structure of the lithiated silane $[(R)\text{-}\mathbf{7}\cdot(t\text{BuLi})]_2$ in the crystal. The numbering scheme of the hydrogen atoms has been omitted for clarity. Selected bond lengths [Å] and angles [°]: C1–Si1 1.835(3), C2–Si1 1.892(3), C1–Li2 2.213(7), C1–Li1′ 2.275(6), C1–Li1 2.299(6), C11–N1 1.477(4), C11–Si1 1.922(3), C17–Li2 2.290(8), C17–Li2′ 2.295(9), C17–Li1 2.471(8), Li1–N1 2.203(7), Li1–C1′ 2.275(6), Li1–Li2 2.512(8), Li1–Li2′ 2.668(8), Li1–Li1′ 2.760(11), Li2–C17′ 2.295(9), Li2–Li2′ 2.419(13), Li2–Li1′ 2.668(8), Si1–Si2 2.3331(15); Si1-C1-Li1 95.4(2), N1-C11-Si1 114.4(2); symmetry operations to generate equivalent atoms: ′: $-x+2$, $-y+1$, z.

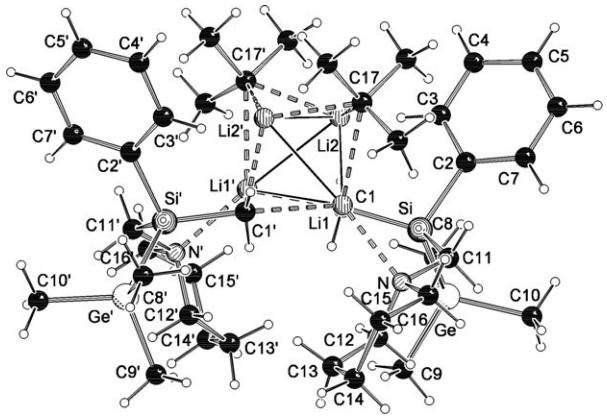

Figure 4. Molecular structure of the lithiated silagermane $[(R)\text{-}\mathbf{10}\cdot(t\text{BuLi})]_2$ in the crystal. The numbering schemes of the hydrogen atoms and some of the carbon atoms have been omitted for clarity. Selected bond lengths [Å] and angles [°]: C1–Si 1.832(5), C2–Si 1.877(5), C11–Si 1.910(5), C1–Li1 2.291(10), C1–Li1′ 2.265(9), C17–Li2 2.263(14), C17–Li2′ 2.266(13), C11–N 1.485(6), Li1–N 2.189(9), Li1–Li2 2.505(12), Li1–Li2′ 2.651(12), Li1–Li1′ 2.747(16), Li2–Li2′ 2.388(19), Li2–Li1′, 2.651(12), Si–Ge 2.3606(18); Si-C1-Li1 95.0(3), N-C11-Si 113.8(3); symmetry operations to generate equivalent atoms: ′: $-x+2$, $-y+1$, z.

silicon center. However, different structures are formed. With an excess of *t*BuLi, the sterically demanding disilane unit is replaced by the smaller *tert*-butyl unit.

Crystallization experiments with the lithiated silagermane *rac*-**10** using one as well as two equivalents of *t*BuLi also resulted in the formation of crystalline solids. However, phase transformations during the selection of the crystals prevented their measurement. Nevertheless, after treatment of the enantiomerically pure silagermane with two equivalents of *t*BuLi, a crystalline solid could be isolated. $[(R)\text{-}\mathbf{10}\cdot(t\text{BuLi})]_2$ crystallized from *n*-pentane in the hexagonal crystal system, space group $P6_4$, and was found to possess the same mixed structure (Figure 4), with two molecules of the silagermane being replaced by smaller *t*BuLi units, as described above for the enantiomerically pure disilane $[(R)\text{-}\mathbf{7}\cdot(t\text{BuLi})]_2$.

The average side length (Li–Li distance) of the central Li_4 tetrahedron is 2.562(13) Å and is therefore in the same range as that of the mixed aggregate of the above-described disilane (2.59(9) Å) and significantly shorter than that of the lithiated disilane without *t*BuLi (2.72(8) Å). The Li–C contacts (2.263(14)–2.291(10) Å) are in the typical range for this class of compounds. In contrast to what was found for the lithiated disilane **7**, only crystals of the mixed aggregate could be identified for the lithiated silagermane, even after the usage of a sub-stoichiometric amount of *t*BuLi. Thus, it seems that the formal substitution of the $SiMe_3$ unit in **3** by the sterically more demanding $GeMe_3$ unit in **6** prevents the crystallization of a structure without incorporated *t*BuLi. Only the exchange of the lithiated silagermane by the smaller *t*BuLi enables the successful crystallization of $[(R)\text{-}\mathbf{10}\cdot(t\text{BuLi})]_2$, even if there is a deficiency of *t*BuLi.

Finally, we also succeeded in isolating the lithiated trisilane $(rac\text{-}\mathbf{12})_2$. The use of either one or two equivalents of *t*BuLi resulted in the formation of the same crystalline solid of the lithiated system. In contrast to the tetrameric structures described above, $(rac\text{-}\mathbf{12})_2$ forms a dimeric structure that does not incorporate *t*BuLi. Evidently, the increased steric demand of the trisilane permits only the formation of this dimeric structure. Its central structural motif consists of an Li–C–Li–C four-membered ring, which, in analogy to those in other dimeric lithium organyls,[24] is slightly deviated from planarity (sum of angles: 357.78°). The Li–C contacts are significantly smaller (2.142(4), 2.175(4) Å) than those in the hitherto discussed lithiated silanes, but they are in the range of monomeric lithium organyls (contacts smaller than 2.20 Å).[22] This can easily be explained with reference to the coordination sphere of the lithium. As shown in Figure 5, the lithium atoms in $(rac\text{-}\mathbf{12})_2$ have a coordination number of only three (cf. four in the lithiated disilane and silagermane). This threefold coordination results in increased cationic character and thus in a stronger electrostatic attraction between the carbanionic carbon and the shortened Li–C contact.

Figure 6 shows the three different structural motifs; Figure 7 summarizes the determined structural motifs of the α-lithiated silanes. Overall, the structure formation is determined by the steric demand of the system and the amount of *t*BuLi used. In general, a structure with a central Li_4 tetrahedron, comparable to that in $(t\text{BuLi})_4$, is preferred. Increasing steric demand results in the formation of mixed aggregates incorporating two lithium organyls, and finally in the formation of a dimeric structure after a further increase in the bulkiness of the substituents at the central silicon.

In each of the isolated systems, the Si–C distance to the lithiated carbon center is the shortest of all of the Si–C distances in the respective molecule {for example, $(rac\text{-}\mathbf{7})_4$:

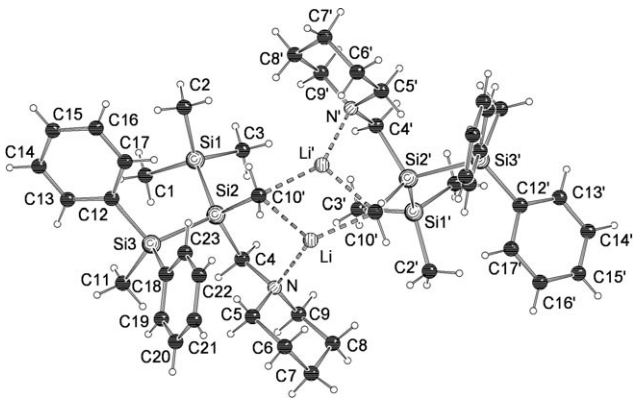

Figure 5. Molecular structure of the lithiated silane (*rac*-**12**)$_2$ in the crystal. The numbering scheme of the hydrogen atoms has been omitted for clarity. Selected bond lengths [Å] and angles [°]: C4–N 1.482(3), C4–Si2 1.930(2), C10–Si2 1.836(2), C10–Li′ 2.142(4), C10–Li 2.175(4), Li–N 2.052(4), Li–C10′ 2.142(4), Li–Li′ 2.348(7), Li–Si2 3.004(4), Si1–Si2 2.3426(12), Si2–Si3 2.3601(12); N-C4-Si2 114.52(14), Si2-C10-Li 96.64(14), N-Li-C10 101.69(17), N-Li-Si2 66.36(11), C10-Li-Si2 37.37(8), C4-N-Li 98.63(16); symmetry operations to generate equivalent atoms: ′: $-x$, y, $-z+1/2$.

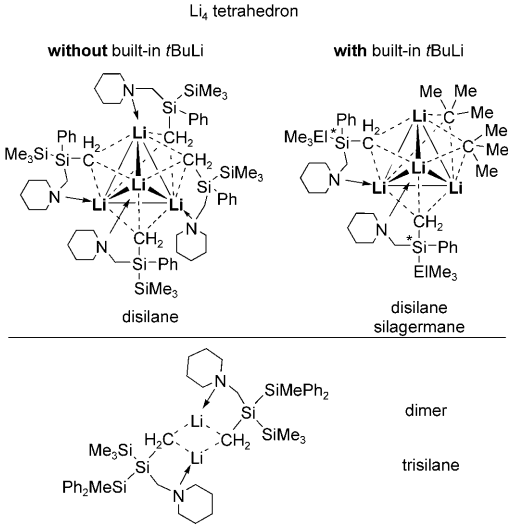

Figure 6. Drawing of the molecular structure of the lithiated silanes; El = Si (disilane) or Ge (silagermane).

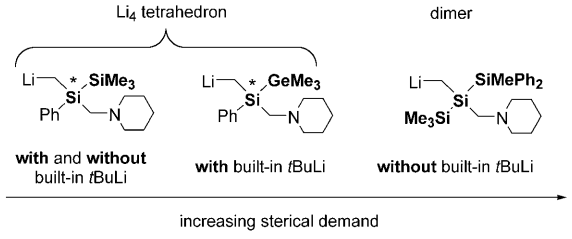

Figure 7. Comparison of the different structural motifs of the lithiated silanes.

1.844(3) Å, [(*R*)-**7**·(*t*BuLi)]$_2$: 1.835(3) Å, [(*R*)-**10**·(*t*BuLi)]$_2$: 1.832(5) Å, (*rac*-**12**)$_2$: 1.836(2) Å}. Such a shortened bond has recently been observed in an α-lithiated benzylsilane and can be attributed to a polarizing effect (α-effect) between the lithiated carbon and the neighboring silicon.[19c] A second similarity of all of the lithiated silanes concerns the aminomethyl side-arm. In all of the determined solid-state structures, the amino side-arm is seen to be coordinated to the adjacent lithium of the Li_4 tetrahedron or of the Li–C–Li–C four-membered ring, respectively. This coordination stabilizes all of the solid-state structures, while, at the same time, is also the reason for the successful deprotonation of these systems, which would otherwise be impossible. This complexation also suggests a pre-coordination of the lithium organyl in the transition state. According to the complex-induced proximity effect (CIP effect), this results in the approach of the reactive groups (alkyllithium base and methyl group) and thus enables the deprotonation.

Theoretical studies: In the experiments, all of the silanes showed selective lithiation of the methyl group at the stereogenic silicon atom, thus indicating a strong preference for this process compared to potential alternative deprotonation reactions. To gain insight into the energetic situation of the deprotonation reactions and to evaluate the different reaction barriers, DFT studies were performed. For example, the deprotonation of disilane **3** at the SiMe group (SiMe-ED, SiMe-TS) and at the $SiMe_3$ group ($SiMe_3$-ED, $SiMe_3$-TS) were calculated (see Figure 8). At first, a monomeric model system was assumed, with *t*BuLi coordinated by the piperidino side-arm (according to the CIP effect[25]) and dimethyl ether present to complete the coordination sphere. Fourfold coordination of the lithium could be excluded due to the spatial overload of the system. The geometries of the stationary points were initially optimized using density functional theory with the hybrid B3LYP functional and the 6-31+G(d) basis set.[26] To identify transition-state structures, frequency calculations were carried out at the same level. Both transition states are depicted in Figure 8.

The calculations on this monomer-based mechanism showed a strong preference for deprotonation of the SiMe group compared to that of the $SiMe_3$ unit. While SiMe-TS has an associated barrier of only 60 kJ mol^{-1}, the deprotonation of the $SiMe_3$ unit requires 84 kJ mol^{-1}. The overall pref-

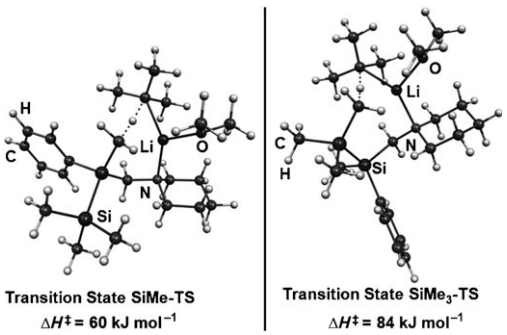

Figure 8. Transition states of the α-lithiation of disilane **3**; selective lithiation of the methyl group (SiMe-TS, left), selective lithiation of the trimethylsilyl group ($SiMe_3$-TS, right), B3LYP/6-31+G(d).

erence of 24 kJ mol^{-1} is consistent with the experimentally observed selective deprotonation. This energy difference can be rationalized in terms of the spatial situations in the corresponding transition states and starting systems. In the starting system of the deprotonation of the $SiMe_3$ group, there is already a strong repulsion between the bulky $SiMe_3$ group and the spatially demanding *tert*-butyl moiety of the organolithium reagent. Approach of the reactants in the transition state leads to a further increase in the repulsion between these groups, thus resulting in the experimentally observed selective deprotonation of the SiMe group. This strong preference is also evident in a dimer-based mechanism. The formation of such a dimeric model system with its Li–C–Li–C four-membered ring is reasonable as numerous organolithium compounds are known to form such dimeric structures. This mechanism was assumed as in the experiments no coordinating solvent was used. The dimeric transition states were modeled with trimethylamine replacing the second piperidino side-arm (see Figure 9). Calculations on this dimer-based mechanism yielded a barrier of only 76 kJ mol^{-1} for deprotonation of the SiMe group. For deprotonation of the $SiMe_3$ group, no stationary point could be located due to the spatial overload of this system. Overall, the calculations are consistent with the experimental observations and account for the observed selectivity in terms of repulsion effects in the corresponding transition states.

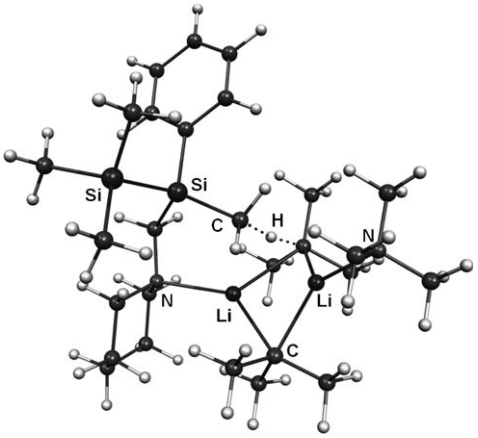

Figure 9. Dimer-based transition state of the α-lithiation of the SiMe group of disilane **3**; B3LYP/6-31+G(d).

Synthesis of α-functionalized, enantiomerically pure silanes by diastereoselective α-lithiation of a dimethylsilane: Having established the conditions for direct deprotonation of methyl-substituted silanes, we tried to expand this reaction to the desymmetrization of a non-chiral silicon center, that is, to the preparation of Si-centered chiral silanes by selective α-lithiation of one specific methyl group of a dimethyl-substituted silane. For this purpose, a silane with a chiral side-arm for the transfer of stereo-information was synthesized. As starting material, we selected the C_2-symmetric chiral (1*R*,2*R*)-*N*,*N*,*N*′,*N*′-tetramethylcyclohexane-1,2-diamine [(*R*,*R*)-TMCDA, (*R*,*R*)-**15**], since it is known to be readily and selectively α-deprotonated at a methyl group, thereby allowing the facile introduction of stereo-information into the molecule.[27,28] Thus, dimethylsilane (*R*,*R*)-**16** was synthesized by a trapping reaction of the α-lithiated (*R*,*R*)-TMCDA with the corresponding chlorosilane (Scheme 6) and was obtained in 62% yield after work-up and distillation.

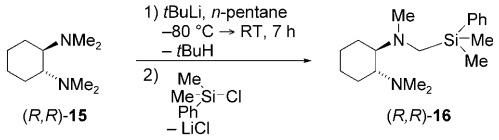

Scheme 6. Synthesis of dimethylsilane (*R*,*R*)-**16** via α-lithiated (*R*,*R*)-TMCDA.

For selective lithiation of the dimethylsilane, a solution of (*R*,*R*)-**16** in *n*-pentane was treated with *tert*-butyllithium at low temperature and the intermediate was trapped with either trimethyl- or tributyltin chloride (Scheme 7). Prior to

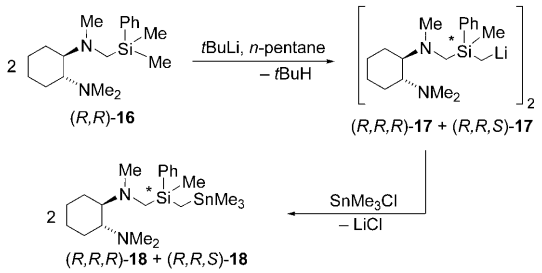

Scheme 7. Asymmetric lithiation of dimethylsilane (*R*,*R*)-**16** and trapping with trimethyltin chloride to afford stannane **18**.

work-up, the reaction mixtures were examined by NMR spectrometry to determine the selectivity of the deprotonation reaction. This revealed diastereoselectivities between 70:30 and 80:20, depending on the reaction temperature (Table 1), with yields of **18** of around 70% after work-up.

Table 1. Reaction conditions and selectivities of the trapping of **17**.

Lithiation/trapping temperature [°C]		*d.r.*
−78 to −70/−70	crystals + solution	70:30
−110 to −75/−75	crystals + solution	74:26
−110 to −78/−78	crystals + solution	80:20
−110 to −78/−78	crystals	80:20

The decrease in selectivity with increasing reaction temperature can be attributed to the kinetic control of such deprotonation reactions. The moderate asymmetric induction of the TMCDA side-arm is in accordance with the low selectivities observed in asymmetric deprotonation reactions mediated by this ligand.[29]

To understand the moderate induction of the amino side-arm used, crystallographic investigations of the intermediate

lithiated silane were performed at different reaction temperatures. From a reaction mixture obtained by carrying out the lithiation at −120 °C and warming to −78 °C, crystals of the diastereomerically pure silane (R,R,S_{Si})-**17** were isolated. In contrast, when deprotonation was carried out at a relatively high temperature (−40 °C), crystals of a 1:1 aggregate of both possible diastereomers were formed upon cooling to −78 °C. The crystal structures of the two different lithiated molecules are depicted in Figures 10 and 11. Figure 12

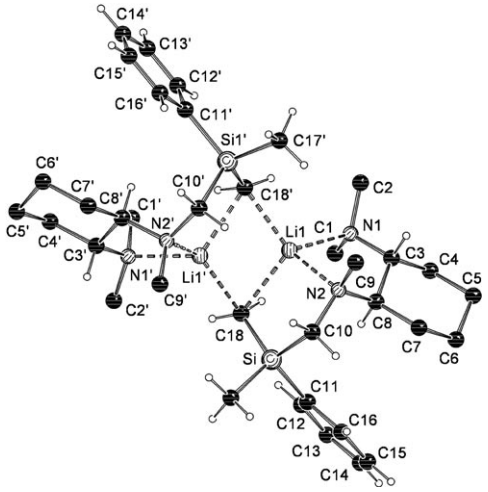

Figure 10. Molecular structure of diastereomerically pure silane (R,R,S_{Si})-**17**. All hydrogen atoms of the amino side-arm except those at the stereogenic carbon centers and those of the solvent molecule have been omitted for clarity. Selected bond lengths [Å] and angles [°]: C17−Si1 1.878(3), C18−Si1 1.787(4), C18−Li1′ 2.190(8), C18−Li1 2.315(6), N1−Li1 2.149(7), N2−Li1 2.137(7), Li1−C18′ 2.190(8), Li1−Li1′ 2.525(13), C10−Si1 1.891(3), C11−Si1 1.893(4); Si1-C18-Li1′ 127.3(3), Si1-C18-Li1 100.3(2), Li1′-C18-Li1 68.1(3), N2-Li1-N1 84.1(3), N2-Li1-C18′ 136.9(3), N2-Li1-C18 95.2(2), N1-Li1-C18 120.6(3), C18′-Li1-C18 109.6(3), Li1′-C18-Li1 68.1(3); symmetry operations to generate equivalent atoms: $-x+1, y, -z+1$.

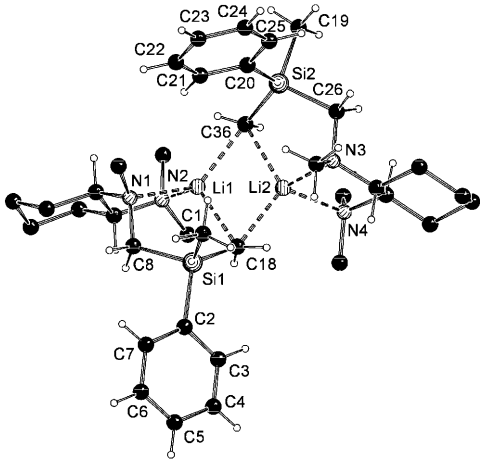

Figure 11. Molecular structure of the 1:1 aggregate of both silane diastereomers (R,R,R_{Si})- and (R,R,S_{Si})-**17**. All hydrogen atoms of the amino side-arm except those at the stereogenic carbon centers and those of the solvent molecule have been omitted for clarity. Selected bond lengths [Å] and angles [°]: C1−Si1 1.877(3), C18−Si1 1.810(3), C8−Si1 1.907(4), C18−Li2 2.199(7), C18−Li1 2.239(6), C19−Si2 1.900(4), C26−Si2 1.910(4), C36−Si2 1.806(4), C36−Li2 2.205(7), C36−Li1 2.271(7), Li1−N1 2.133(6), Li1−N2 2.152(6), Li2−N3 2.068(6), Li2−N4 2.194(6); Li2-C36-Li1 67.4(2), Li2-C18-Li1 68.1(2), C18-Li1-C36 109.7(3), C18-Li2-C36 113.8(3).

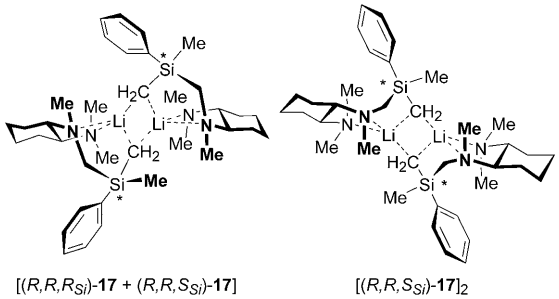

Figure 12. Molecular structures of racemic silanes (R,R,R_{Si})- and (R,R,S_{Si})-**17**.

shows a schematic representation of both structures. Both the diastereomerically pure product and the 1:1 aggregate of the two diastereomers of the lithiated silane form dimeric compounds in the crystal. The pure silane (R,R,S_{Si})-**17** crystallizes in the monoclinic crystal system, space group $C2$, while the 1:1 aggregate crystallizes in the orthorhombic crystal system, space group $P2_12_12_1$. Both molecular structures include an additional solvent molecule (pentane, hexane). The asymmetric unit of the 1:1 aggregate contains one molecule of the dimer, while that of the diastereomerically pure compound contains only one half of the dimer, which is assembled to the dimer through C_2 symmetry. The central structural motif of both dimers is formed by an Li–C–Li–C four-membered ring, as has been observed in the case of *rac*-**12**, and is typical of dimeric alkyllithium compounds.[22,24] The lithium atoms exhibit fourfold coordination, with contacts to the metalated carbon atoms and both nitrogen atoms of the diamino side-arm. The Li–C distances vary between 2.190(8) and 2.315(13) Å in the (R,R,S_{Si})-silane and between 2.199(7) and 2.271(7) Å in the aggregate, and are thus comparable to those in known oligomeric organolithiums.[22,24] The same is true for the lithium–nitrogen contacts. The silicon atoms have tetrahedral coordination spheres, with almost ideal angles ranging from 102.2(2) to 116.0(2)°. However, the Si–C distances vary significantly, with the shortest contacts to the lithiated carbon atoms ((R,R,S_{Si})-silane: 1.787(4) Å; 1:1 aggregate: 1.810(3) and 1.806(4) Å). This shortening has already been observed in the α-lithiated oligosilanes (see above) and can be attributed to the polarizing effect (α-effect) between the lithiated carbon and the silicon.[19c]

The fact that the diastereomerically pure lithiated intermediate could be isolated from the reaction mixture prompted us to investigate whether an increase in the diastereoselectivity might be achieved by carrying out a trapping reaction with exclusively the crystalline solid. However, after work-up, the same diastereomeric ratio (80:20) was obtained as with the whole reaction mixture. This indicated

that both the (R,R,S_{Si})-silane and the 1:1 aggregate were present in the solid and that no enrichment of the selectivity could be achieved by crystallization.

Theoretical studies of the diastereoselective α-lithiation: To gain insight into the mechanistic features of the asymmetric deprotonation of dimethylsilane (R,R)-**16**, computational studies were performed to evaluate the reaction barriers associated with lithiations of both diastereotopic methyl groups. For the deprotonation, a mechanism comparable to that for the piperidinomethyl-substituted silane **3** involving a pre-coordinated species was assumed, in accordance with the complex-induced proximity effect (CIPE).[25] As a model system, the monomeric adduct (R,R)-**19** was chosen, in which the *tert*-butyllithium molecule is pre-coordinated by the (R,R)-TMCDA moiety. The formation of such an intermediate during the lithiation reaction is reasonable, as an analogous monomeric *t*BuLi·(R,R)-TMCDA adduct is formed during the deprotonation reaction of the amine itself.[24] In adduct **19**, the nitrogen atom of the side-arm becomes stereogenic upon pre-coordination of the alkyllithium, so that different isomers have to be considered for the calculation of the transition states (**19**-TS) as well as of the pre-coordinated adducts **19**. In the experimentally observed intermediate α-lithiated silanes (R,R,R_{Si})- and (R,R,S_{Si})-**17**, there is no distinct preference for one configuration. While the diastereomerically pure (R,R,S_{Si})-**17** (Figure 10) exhibits an S_N configuration, the nitrogen of the 1:1 aggregate of both diastereomers (Figure 11) has an R_N configuration. In the S_N configuration, the sterically more demanding silyl substituent adopts the pseudo-equatorial position of the five-membered ring that is formed upon the coordination of *t*BuLi.

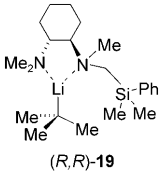

(R,R)-**19**

First, we performed DFT studies on the transition states at the B3LYP/6-31+G(d) level. In principle, two transition states have to be considered for both diastereomeric products (R,R,S_{Si})-**17** and (R,R,R_{Si})-**17**, which differ in the configuration at this stereogenic nitrogen (R_N and S_N). Additionally, further conformers are possible by rotation of the NCH_2Si moiety. For each diastereomer (R_{Si} and S_{Si}), three respective conformers and isomers were calculated. Further conformers could be neglected due to strong repulsion of particular groups. For some of these structures, preliminary calculations at a lower level did not even show a stationary point. Figure 13 depicts the four most favored transition states (two for each diastereomer of **17**), which additionally differ in the configuration at the nitrogen atom. The calculations showed that the three transition states all had energies in the same range, albeit with the most favored one, (R_{Si},R_N)-**19**-TS, leading to the R_{Si}-configured product. At first glance, this seems to be in contradiction to the experiments, whereby the S_{Si} product was probably the main isomer, as this could be isolated from the diastereomerically enriched crystallization medium. However, one also has to consider the configuration at the nitrogen. While the R_N-configured transition states (Figure 13, lower part) show an energetic difference of only 2 kJ mol^{-1}, their S_N-configured counterparts differ in energy by 9 kJ mol^{-1} (Figure 13, upper part). This suggests that with the R_N configuration, the reaction leading to both diastereomers, that is, the formation of a 1:1 mixture of (R,R,S_{Si})-**17** and (R,R,R_{Si})-**17**, may be expected. On the contrary, the S_N configuration would lead to a preference for the silane (R,R,S_{Si})-**17**. Most interestingly, these calculated results on the isomeric transition states are consistent with the molecular structures of **17**. Thus, the diastereomerically pure silane (R,R,S_{Si})-**17** showed selective S_N configuration with regard to the conformation of the silyl unit, which was also identified as the most favored configuration from the theoretical point of view. On the contrary, the 1:1 aggregate of the two diastereomers of **17** exhibited selective R_N config-

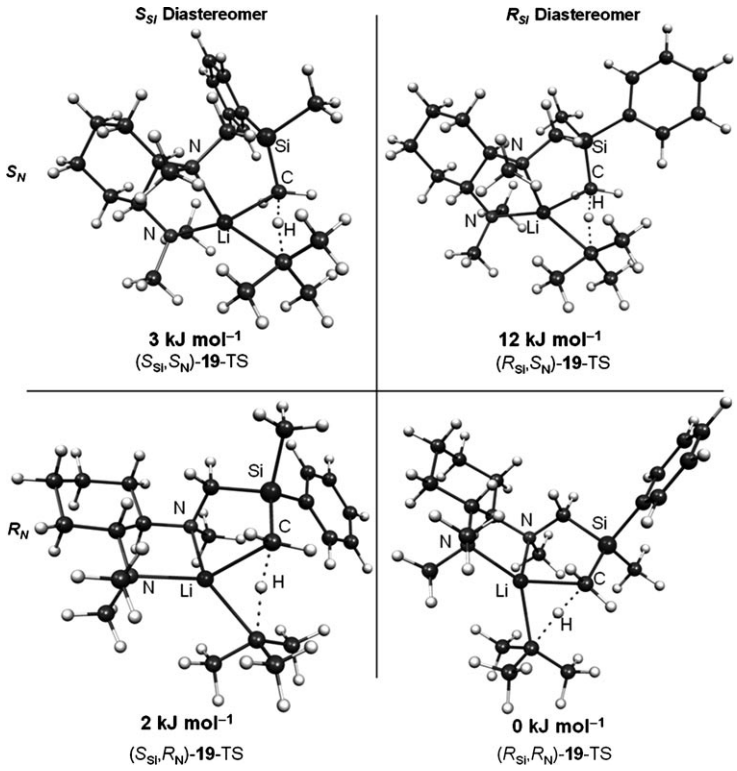

Figure 13. Calculated structures and energies of the diastereomeric transition states of the α-lithiation of the two methyl groups of dimethylsilane (R,R)-**16**, B3LYP/6-31+G(d).

uration. Again, the conformations of the R_{Si}- and S_{Si}-silanes were in accordance with the calculated structures.

Consequently, the experimental and theoretical observations suggest that the stereochemical outcome of the α-lithiation of silane (*R*,*R*)-**16** is determined by the configuration of the stereogenic nitrogen atom of the pre-coordinated *t*BuLi adduct **19**. As the diastereomeric reaction pathways are associated with almost identical reaction barriers, this simultaneously implies that the greater the energetic difference between the R_N and S_N configurations of **19**, the higher the diastereoselectivity of the deprotonation. Subsequent DFT calculations (at the B3LYP/6-31+G(d) level) of the different isomers of **19** revealed a preference of 3 kJ mol^{-1} for the R_N configuration. Again, calculations were performed on several conformers (see the Supporting Information). The three most favored isomers are depicted in Figure 14.

Overall, the energy difference of 3 kJ mol^{-1} between the R_N and S_N configurations of **19** is the crucial criterion for the stereochemical outcome of the deprotonation. This small difference of 3 kJ mol^{-1} befits the moderate selectivities observed experimentally. The low reaction barriers of around 60 kJ mol^{-1} confirm that the α-lithiation will proceed even at low reaction temperatures. Additional calculations taking into account dispersion effects by using the M052X functional and the 6-31+G(d) basis set were indicative of the same tendencies as the DFT calculations, albeit with an elevated preference ($\Delta H = 9$ kJ mol^{-1}) for the R_N configuration (see the Supporting Information). The energies obtained are also listed in Table 2. Again, the most favored isomers and conformers have the same structures as those observed in the isolated crystals. The calculated transition states also point to the formation of a 1:1 mixture ($\Delta\Delta H^{\neq} = 2$ kJ mol^{-1}) via the R_N-configured intermediate **19** and a preference for the S_{Si}-diastereomer **17** ($\Delta\Delta H^{\neq} = 15$ kJ mol^{-1}) when starting from the S_N-configured adduct **19**. Contrary to the calculations using the B3LYP functional, the transition state leading to the S_{Si}-silane showed the lowest barrier ($\Delta H^{\neq} =$ 56 kJ mol^{-1}) under the consideration of dispersion effects. The energetic features of the α-lithiation of silane (*R*,*R*)-**16** are summarized in Figure 15. Overall, the calculations reflect the experimental observations (moderate selectivities, path of the reaction) rather well. The apparent impact of the configuration at the stereogenic nitrogen atom on the stereoselectivity suggests that higher selectivities may be achieved by using dimethylsilanes for which there are higher energy differences between the isomers of the pre-coordinated *t*BuLi adducts.

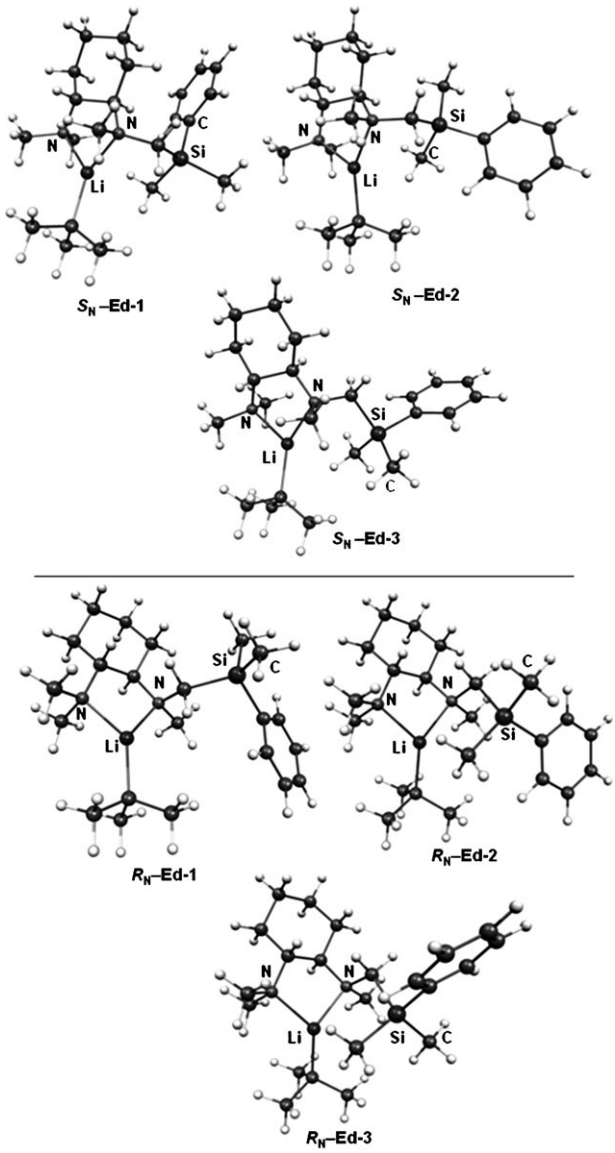

Figure 14. Calculated structures of the isomers and conformers of the pre-coordinated *t*BuLi adduct **19**, B3LYP/6-31+G(d).

Table 2. Relative energies [kJ mol^{-1}] of the isomers and conformers of the precoordinated *t*BuLi adduct **19**.

Compound	B3LYP/6-31+G(d)	M052X/6-31+G(d)
S_N-Ed-1	0	0
S_N-Ed-2	4	8
S_N-Ed-3	8	14
R_N-Ed-1	5	9
R_N-Ed-2	14	24
R_N-Ed-3	3	19

Conclusion

In conclusion, we have presented the direct α-lithiation of methylsilanes as a powerful and efficient method for the generation of Si-chiral compounds. Firstly, this method has been successfully applied to the functionalization of already Si-chiral silanes. In this approach, all of the examined oligosilanes and silagermanes were selectively deprotonated at the stereogenic silicon center. Computational studies have pointed to a mechanism involving pre-complexation of the alkyllithium by the piperidinomethyl side-arm and the induction of regioselectivity due to repulsion effects in the corresponding transition states. The crystal structures of the

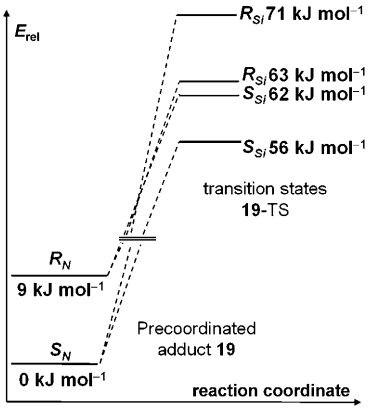

Figure 15. Energetic features of the α-lithiation of silane (*R*,*R*)-**16**, M052X/6-31+G(d).

corresponding α-lithiated silanes exhibit interesting structural motifs and types of aggregation. These have been found to be crucially influenced by the spatial demand of the silane and the amount of alkyllithium used, with the formation of mixed aggregates incorporating *tert*-butyllithium being observed. Secondly, direct deprotonation has also been applied to the formation of Si-chiral compounds by desymmetrization of dimethylsilanes. Here, the use of a chiral (*R*,*R*)-TMCDA side-arm resulted in moderate diastereoselectivities. On the basis of X-ray analyses and computational studies, the observed selectivities may be ascribed to the formation of a stereogenic nitrogen center upon the pre-coordination of the alkyllithium to the silane. The greater the energetic difference between the different configurations of the stereogenic nitrogen, the more selective the reaction. We are currently seeking to optimize the diastereoselective deprotonation by varying the substituents and the chiral side-arm of the silane.

Experimental Section

Experimental details: All experiments were carried out under a dry, oxygen-free argon atmosphere using standard Schlenk techniques. The solvents used were dried over sodium and distilled prior to use. (*R*,*R*)-TMCDA was prepared according to a literature method.[30] ^{1}H, ^{13}C, and ^{29}Si NMR spectra were recorded on Bruker DRX-300 and AMX-500 spectrometers at 22 °C. Signal assignments were corroborated with the aid of additional DEPT-135, C,H-COSY, and H,H-COSY experiments. All chemical shifts are given in ppm on the δ scale. All spin-spin coupling constants (J) are given in Hertz (Hz).

Synthesis of *rac*-8: A solution of *rac*-**3** (1.00 g, 3.43 mmol) in *n*-pentane (10 mL) was combined with a 1.7 M solution of *t*BuLi in *n*-pentane (2.04 mL, 3.45 mmol) at −78 °C. After warming to room temperature, the reaction mixture was stirred for 5 h. Thereafter, one equivalent of Me_3SnCl (0.69 g, 3.45 mmol) was added at −78 °C and the solution was allowed to warm to room temperature once more. After removal of all volatiles in vacuo, the residue was suspended in 2 M NaOH (35 mL) and extracted with diethyl ether (5×30 mL). The combined organic layers were extracted with 2 M HCl (5×20 mL) and the combined aqueous layers were subsequently adjusted to pH 12 with NaOH. Finally, the aqueous layer was extracted with diethyl ether (5×30 mL) and the combined organic layers were dried over Na_2SO_4. After removal of all volatile compounds in vacuo, the crude product was purified by bulb-to-bulb distillation (oven temperature: 171 °C, pressure: 2.2×10^{-5} mbar); yield: 1.19 g, 2.62 mmol (77 %). ^{1}H NMR (500.1 MHz, C_6D_6): $\delta=0.18$ (m, 1H; $SiCH_2Sn$), 0.21 (s, $^2J_{H,^{117}Sn}=25.8$ Hz, $^2J_{H,^{119}Sn}=27.0$ Hz, 9H; $Sn(CH_3)_3$), 0.23 (m, 1H; $SiCH_2Sn$), 0.28 (s, 9H; $Si(CH_3)_3$), 1.30–1.40 (m, 2H; $NCCCH_2$), 1.50–1.60 (m, 4H; $NCCH_2C$), 2.35–2.45 (m, 4H; NCH_2CC), 2.35, 2.50 (AB system, $^2J_{AB}=14.2$ Hz, 2H; $SiCH_2N$), 7.25–7.35 (m, 3H; arom. H-*m*, H-*p*), 7.58–7.62 ppm (m, 2H; arom. H-*o*); {^{1}H}^{13}C NMR (125.8 MHz, C_6D_6): $\delta=-10.23$ (1C; $SiCH_2Sn$), −7.15 ($^1J_{^{13}C,^{117}Sn}=158.2$ Hz, $^1J_{^{13}C,^{119}Sn}=165.5$ Hz, 3C; $Sn(CH_3)_3$), −1.35 (3C; $Si(CH_3)_3$), 24.2 (1C; $NCCCH_2$), 26.6 (2C; $NCCH_2C$), 49.7 (1C; $SiCH_2N$), 59.1 (2C; NCH_2CC), 128.1 (2C; C-*m*, C_6H_5), 128.6 (1C; C-*p*, C_6H_5), 134.2 (2C; C-*o*, C_6H_5), 140.3 ppm (1C; C-*i*, C_6H_5); {^{1}H}^{29}Si NMR (99.4 MHz, C_6D_6): $\delta=-19.2$ (1Si; $SiCH_2N$), −18.9 ppm (1Si; $Si(CH_3)_3$); GC/EI-MS: $t_R=8.20$ min [80 °C (2 min)–10 °C min^{-1}–280 °C (5 min)]; m/z (%): 455 (1) [M^+], 440 (1) [$M-CH_3^+$], 382 (6) [$M-Si(CH_3)_3^+$], 290 (1) [$M-Sn(CH_3)_3^+$], 207 (3) [$M-CH_2Sn(CH_3)_3^+$]$^+$, 165 (2) [$Sn(CH_3)^+$], 98 (100) [($H_2C{=}NC_6H_5$)$^+$], 73 (1) [$Si(CH_3)^+$]; elemental analysis (%) calcd for $C_{19}H_{37}NSi_2Sn$: C 50.2, H 8.21, N 3.08; found: C 50.6, H 8.41, N 3.19.

Determination of the enantiomeric ratio of *rac*-8 with (*R*)-mandelic acid: The enantiomeric ratio was determined in the presence of three equivalents of (*R*)-mandelic acid. Therefore, *rac*-**8** (15.0 mg, 33.0 μmol) was added to a solution of (*R*)-mandelic acid (15.1 mg, 99.0 μmol) in $CDCl_3$ (500 μL). ^{1}H NMR (500.1 MHz, C_6D_6): $\delta=-0.13$ (m, 1H; $SiCH_2Sn$, D1), −0.11 (m, 1H; $SiCH_2Sn$, D2), −0.08 (s, 9H; $Sn(CH_3)_3$, D1), −0.06 (s, 9H; $Sn(CH_3)_3$, D2), −0.23 (m, 1H; $SiCH_2Sn$, D1), −0.01 (m, 1H; $SiCH_2Sn$, D2), 0.34 (s, 9H; $Si(CH_3)_3$, D2), 0.41 (s, 9H; $Si(CH_3)_3$, D1), 1.20–1.35 (m, 4H; $NCCCH_2$, D1 & D2), 1.40–1.60 (m, 8H; $NCCH_2C$, D1 & D2), 2.35–2.45, 2.50–2.65 (m, 6H each; NCH_2CC & $SiCH_2N$, D1 & D2), 4.85 (s, 2H; C*H*OH), 7.25–7.35 (m, 6H; arom. H-*m*, H-*p*), 7.58–7.62 ppm (m, 4H; arom. H-*o*); OH, NH not located; {^{1}H}^{13}C NMR (125.8 MHz, C_6D_6): $\delta=-10.8$ (2C; $SiCH_2Sn$, D1 & D2), −7.2 (6C, $^1J_{^{13}C,^{117}Sn}=161.6$ Hz, $^1J_{^{13}C,^{119}Sn}=168.0$ Hz; $Sn(CH_3)_3$, D1 & D2), −1.38, −1.36 (3C each, $^1J_{^{13}C,^{29}Si}=21.8$ Hz; $Si(CH_3)_3$, D1 & D2), 22.4 (2C; $NCCCH_2$, D1 & D2), 23.8 (4C; $NCCH_2C$, D1 & D2), 48.9 (2C; $SiCH_2N$, D1 & D2), 57.0 (4C; NCH_2CC, D1 & D2), 74.3 (2C; CHOH), 126.5 (4C; C-*m*, C_6H_5CHOH), 126.7 (2C; C-*p*, C_6H_5CHOH), 127.8 (4C; C-*o*, C_6H_5CHOH), 128.0 (4C; C-*m*, C_6H_5Si), 129.0 (2C; C-*p*, C_6H_5Si), 134.1 (4C; C-*o*, C_6H_5Si), 137.1 (2C; *C*-i, C_6H_5Si), 142.7 (2C; C-*i*, C_6H_5CHOH), 177.7 ppm (2C; COO); {^{1}H}^{29}Si NMR (99.4 MHz, C_6D_6): $\delta=-20.0$ (2Si; $SiCH_2N$), −19.12, −19.10 ppm (1Si each; $Si(CH_3)_3$, D1 & D2).

Synthesis of (*R*)-8: The synthesis of (*R*)-**8** was analogous to that of *rac*-**8**. The analytical data of the product were consistent with those of *rac*-**8**. Yield: 1.35 g, 2.96 mmol, 86 %; $[\alpha]_D^{20}=24.5$ ($c=0.40$ in cyclohexane).

Determination of the enantiomeric ratio of (*R*)-8 with (*R*)-mandelic acid: The enantiomeric ratio was determined in the presence of three equivalents of (*R*)-mandelic acid. Therefore, (*R*)-**8** (15.0 mg, 33.0 μmol) was added to a solution of (*R*)-mandelic acid (15.1 mg, 99.0 μmol) in $CDCl_3$ (500 μL). ^{1}H NMR (500.1 MHz, C_6D_6): $\delta=-0.13$ (m, 1H; $SiCH_2Sn$), −0.08 (s, 9H; $Sn(CH_3)_3$), −0.23 (m, 1H; $SiCH_2Sn$), 0.05 (s, 9H; $Si(CH_3)_3$), 1.20–1.35 (m, 2H; $NCCCH_2$), 1.40–1.60 (m, 4H; $NCCH_2C$), 2.35–2.65 (m, 6H; NCH_2CC & $SiCH_2N$), 4.84 (s, 1H; C*H*OH), 7.30–7.35 (m, 3H; arom. H-*m*, H-*p*), 7.40–7.45 ppm (m, 2H; arom. H-*o*); OH and NH not located; {^{1}H}^{13}C NMR (125.8 MHz, C_6D_6): $\delta=-10.9$ (1C; $SiCH_2Sn$), −7.2 (3C, $^1J_{^{13}C,^{117}Sn}=161.8$ Hz, $^1J_{^{13}C,^{119}Sn}=169.1$ Hz; $Sn(CH_3)_3$), −1.36 (3C, $^1J_{^{13}C,^{29}Si}=22.8$ Hz; $Si(CH_3)_3$), 22.1 (1C; $NCCCH_2$), 23.4 (2C; $NCCH_2C$), 48.8 (1C; $SiCH_2N$), 56.7 (2C; NCH_2CC), 74.3 (1C; CHOH), 126.4 (2C; C-*m*, C_6H_5CHOH), 126.6 (C-*p*, C_6H_5CHOH), 127.8 (2C; C-*o*, C_6H_5CHOH), 128.1 (2C; C-*m*, C_6H_5Si), 129.1 (1C; C-*p*, C_6H_5Si), 133.8 (1C; C-*i*, C_6H_5CHOH), 134.1 (2C; C-*o*, C_6H_5Si), 137.0 (1C; C-*i*, C_6H_5Si), 177.5 ppm (1C; COO); {^{1}H}^{29}Si NMR (99.4 MHz, C_6D_6): $\delta=-20.1$ (1Si; $SiCH_2N$), −19.1 (1Si; $Si(CH_3)_3$); e.r. > 99:1.

Synthesis of *rac*-9: A solution of *rac*-**3** (2.50 g, 8.57 mmol) in *n*-pentane (15 mL) was combined with a 1.5 M solution of *t*BuLi in *n*-pentane (6.28 mL, 9.43 mmol, 1.1 equiv) at −78 °C. After warming to room temperature, the reaction mixture was stirred for 5 h. Thereafter, one equivalent of paraformaldehyde (283 mg, 9.43 mmol) was added at −78 °C and

the solution was allowed to warm to room temperature once more and stirred for 24 h. After the addition of H_2O (169 mg, 9.43 mmol) and stirring for 24 h, all volatiles were removed in vacuo, and the residue was suspended in a mixture of *n*-pentane (12 mL) and diethyl ether (15 mL) and freed of all salts. After the removal of all volatile compounds in vacuo, *rac*-**9** could be isolated. Yield: 2.66 g, 8.27 mmol (85%). ^{1}H NMR (300.1 MHz, C_6D_6): $\delta = 0.16$ (s, 9H; $Si(CH_3)_3$), 1.20–1.30 (m, 2H; $NCCCH_2$), 1.45–1.60 (m, 4H; $NCCH_2C$), 1.55–1.60 (m, 2H; $SiCH_2CH_2OH$), 2.25–2.40 (m, 4H; NCH_2CC), 2.01, 2.12 (AB system, $^2J_{AB} = 14.4$ Hz, 2H; $SiCH_2N$), 4.17 (br, 2H; $SiCH_2CH_2OH$), 6.30–6.40 (br, 1H; $SiCH_2CH_2OH$), 7.20–7.35 (m, 3H; arom. H), 7.45–7.55 ppm (m, 2H; arom. H); {^{1}H}^{13}C NMR (75.5 MHz, $CDCl_3$): $\delta = -1.8$ (3C; $Si(CH_3)_3$), 16.6 (1C; $SiCH_2CH_2OH$), 23.8 (1C; $NCCCH_2$), 25.9 (2C; $NCCH_2C$), 46.7 (1C; $SiCH_2N$), 58.3 (2C; NCH_2CC), 58.5 (1C; $SiCH_2CH_2OH$), 128.2 (2C; C-*m*, C_6H_5), 128.8 (1C; C-*p*, C_6H_5), 134.2 (2C; C-*o*, C_6H_5), 137.4 ppm (1C; C-*i*, C_6H_5); {^{1}H}^{29}Si NMR (59.6 MHz, $CDCl_3$): $\delta = -21.8$ (1Si; $SiCH_2N$), −19.1 ppm (1Si; $Si(CH_3)_3$).

Determination of the enantiomeric ratio of *rac*-9 with [Eu(hfc)$_3$]: The enantiomeric ratio was determined in the presence of an excess of tris[3-(heptafluoropropylhydroxymethylene)-(+)-camphorato]europium(III), [Eu(hfc)$_3$]. Therefore, *rac*-**8** (15.0 mg, 46.6 μmol) was added to a solution of [Eu(hfc)$_3$] (30 mg) in $CDCl_3$ (500 μL). ^{1}H NMR (300.1 MHz, $CDCl_3$): $\delta = 0.32$ (s, 9H; $Si(CH_3)_3$, D2), 0.33 (s, 9H; $Si(CH_3)_3$, D1), 1.00–1.10 (m, 2H; $SiCH_2CH_2OH$, D1), 1.30–1.40 (m, 2H; $NCCH_2C$, D2), 1.45–1.55 (m, 4H; $NCCCH_2$, D1 & D2), 1.50–1.55 (m, 2H; $SiCH_2CH_2OH$, D2), 1.55–1.65 (m, 2H; $NCCH_2C$, D1), 1.95–2.10 (m, 4H; $NCCH_2C$, D1 & D2), 2.35–2.45 (m, 8H; NCH_2CC), 2.95–3.15 (D2), 3.15–3.25 (D1) (m, 2H each; $SiCH_2N$), 3.70–4.20 (br, 4H; $SiCH_2CH_2OH$, D1 & D2), 7.30–7.55 (m, 6H; arom. H), 7.85–7.95 ppm (m, 4H; arom. H); OH not located; {^{1}H}^{13}C NMR (75.5 MHz, $CDCl_3$): $\delta = -1.78$ (D1), −1.77 (D2) (3C each; $Si(CH_3)_3$), 16.9 (1C; $SiCH_2CH_2OH$, D2), 17.2 (1C; $SiCH_2CH_2OH$, D1), 24.12 (2C; $NCCCH_2$, D1 & D2), 26.37 (D1), 26.43 (D2) (2C each; $NCCH_2C$), 47.4 (D1), 47.5 (D2) (1C each; $SiCH_2N$), 58.7 (2C; $SiCH_2CH_2OH$, D1 & D2), 59.2 (D2), 59.3 (D1) (2C each; NCH_2CC), 128.1 (D1), 128.3 (D2) (2C each; C-*m*, C_6H_5), 128.51 (D2), 128.57 (D1) (1C each; C-*p*, C_6H_5), 134.45 (D2), 134.53 (D1) (2C each; C-*o*, C_6H_5), 137.6 (D2), 137.7 ppm (D1) (1C each; C-*i*, C_6H_5); {^{1}H}^{29}Si NMR (59.6 MHz, $CDCl_3$): $\delta = -20.9$ (1Si; $SiCH_2N$, D1), −20.7 (1Si; $SiCH_2N$, D2), −19.1, −19.0 ppm (1Si each; $Si(CH_3)_3$, D1 & D2).

Synthesis of (*R*)-9: The synthesis of (*R*)-**9** was analogous to that of *rac*-**9**. The analytical data of the product were consistent with those of *rac*-**9**. Yield: 950 mg, 2.95 mmol, 91%; $[\alpha]_D^{20} = 10.0$ ($c = 0.30$ in cyclohexane).

Determination of the enantiomeric ratio of (*R*)-9 with [Eu(hfc)$_3$]: The enantiomeric ratio was determined in the presence of an excess of tris[3-(heptafluoropropylhydroxymethylene)-(+)-camphorato]europium(III), [Eu(hfc)$_3$]. Therefore, (*R*)-**8** (15.0 mg, 46.6 μmol) was added to a solution of [Eu(hfc)$_3$] (30 mg) in $CDCl_3$ (500 μL). ^{1}H NMR (300.1 MHz, $CDCl_3$): $\delta = 0.40$ (s, 9H; $Si(CH_3)_3$), 0.95–1.05 (m, 2H; $SiCH_2CH_2OH$), 1.45–1.55 (m, 2H; $NCCCH_2$), 1.55–1.70, 1.85–2.00 (m, 2H each; $NCCH_2C$), 2.15–2.35 (m, 4H; NCH_2CC), 2.95–3.15 (m, 2H; $SiCH_2N$), 3.40–3.60 (br, 2H; $SiCH_2CH_2OH$), 7.45–7.60 ppm (m, 5H; arom. H); OH not located; {^{1}H}^{13}C NMR (75.5 MHz, $CDCl_3$): $\delta = -1.64$ (3C; $Si(CH_3)_3$), 18.1 (1C; $SiCH_2CH_2OH$), 24.2 (1C; $NCCCH_2$), 26.8 (2C; $NCCH_2C$), 48.1 (1C; $SiCH_2N$), 58.9 (1C; $SiCH_2CH_2OH$), 59.7 (2C; NCH_2CC), 128.7 (2C; C-*m*, C_6H_5), 129.2 (1C; C-*p*, C_6H_5), 134.8 (2C; C-*o*, C_6H_5), 138.0 ppm (1C; C-*i*, C_6H_5); {^{1}H}^{29}Si NMR (59.6 MHz, $CDCl_3$): $\delta = -19.9$ (1Si; $SiCH_2N$), −18.5 ppm (1Si; $Si(CH_3)_3$); e.r. > 99:1.

Synthesis of (*R*)-11: The synthesis of (*R*)-**11** was analogous to that of (*R*)-**8**. The crude product was purified by bulb-to-bulb distillation (oven temperature: 170 °C, pressure: 1.0×10^{-3} mbar); yield: 705 mg, 1.41 mmol (95%). ^{1}H NMR (500.1 MHz, C_6D_6): $\delta = 0.24$ (s, $^1J_{H,^{117}Sn} = 158.8$ Hz, $^1J_{H,^{119}Sn} = 166.2$ Hz, 9H; $Sn(CH_3)_3$), 0.26, 0.30 (s, 1H each; $SiCH_2Sn$), 0.45 (s, 9H; $Ge(CH_3)_3$), 1.35–1.40 (m, 2H; $NCCCH_2$), 1.55–1.60 (m, 4H; $NCCH_2C$), 2.41, 2.54 (AB system, $^2J_{AB} = 14.3$ Hz, 2H; $SiCH_2N$), 2.40–2.50 (m, 4H; NCH_2CC), 7.30–7.35 (m, 3H; arom. H-*m*, H-*p*), 7.60–7.65 ppm (m, 2H; arom. H-*o*); {^{1}H}^{13}C NMR (125.8 MHz, C_6D_6): $\delta = -9.74$ (1C; $SiCH_2Sn$), −7.23 (3C; $^1J_{^{13}C,^{117}Sn} = 158.8$ Hz, $^1J_{^{13}C,^{119}Sn} = 166.2$ Hz; $Sn(CH_3)_3$), −1.95 (3C; $Ge(CH_3)_3$), 24.2 (1C; $NCCCH_2$), 26.6 (2C; $NCCH_2C$), 49.8 (1C; $SiCH_2N$), 59.0 (2C; NCH_2CC), 128.1 (2C; C-*m*, C_6H_5Si), 128.8 (1C; C-*p*, C_6H_5Si), 134.1 (2C; C-*o*, C_6H_5Si), 139.9 ppm (1C; C-*i*, C_6H_5Si); {^{1}H}^{29}Si NMR (99.4 MHz, C_6D_6): $\delta = -12.4$ ppm (1Si; $SiCH_2N$); GC/EI-MS: $t_R = 9.99$ min [80 °C (2 min)–10 °C min^{-1}–280 °C (5 min)]; *m*/*z* (%): 486 (1) [$(M-Me)^+$], 382 (30) [$(M-Sn)^+$], 98 (100) [$(H_2C{=}NC_5H_8)^+$]; elemental analysis (%) calcd for $C_{19}H_{37}NSiGeSn$: C 45.7, H 7.48, N 2.81; found: C 46.2, H 7.65, N 2.97.

Synthesis of *rac*-13: The synthesis of *rac*-**13** was analogous to that of *rac*-**8**. The residue was suspended in *n*-pentane (10 mL) and freed of all salts. Thereafter, the crude product was purified by bulb-to-bulb distillation (oven temperature: 220 °C, pressure: 1.0×10^{-3} mbar); yield: 79.0 mg, 0.19 mmol (79%). ^{1}H NMR (300.1 MHz, C_6D_6): $\delta = 0.22$ (s, 9H; $Si(CH_3)_3$), 0.43 (t, $^1J_{HD} = 2.01$ Hz, 2H; $SiCH_2D$), 0.87 (s, 3H; $SiSiSiCH_3$), 1.30–1.40 (m, 2H; $NCCCH_2$), 1.50–1.60 (m, 4H; $NCCH_2C$), 2.33 (d, $^2J_{AB} = 1.28$ Hz, 2H; $SiCH_2N$), 2.35–2.40 (m, 4H; NCH_2CC), 7.30–7.40 (m, 6H; arom. H-*m*, H-*p*), 7.75–7.80, 7.80–7.85 ppm (m, 2H each; arom. H-o); {^{1}H}^{13}C NMR (75.5 MHz, C_6D_6): $\delta = -6.88$ (t, $^1J_{CD} = 18.7$ Hz, 1C; $SiCH_2D$), −3.00 (1C; $SiCH_3$), −0.70 (3C; $Si(CH_3)_3$), 24.2 (1C; $NCCCH_2$), 26.6 (2C; $NCCH_2C$), 48.9 (1C; $SiCH_2N$), 58.8 (2C; NCH_2CC), 128.12, 128.13 (2C each; C-*m*, C_6H_5Si), 129.03, 129.04 (1C each; C-*p*, C_6H_5Si), 135.39, 135.51 (2C each; C-*o*, C_6H_5Si), 138.09, 138.19 ppm (1C each; C-*i*, C_6H_5Si); {^{1}H}^{29}Si NMR (59.6 MHz, C_6D_6): $\delta = -46.6$ (1Si; $SiCH_2D$), −18.7 (1Si; $SiCH_3$), −15.4 ppm (1Si; $Si(CH_3)_3$); GC/EI-MS: $t_R = 11.35$ min [80 °C (2 min)–10 °C min^{-1}–280 °C (5 min)]; *m*/*z* (%): 412 (1) [M^+], 397 (2) [$(M-Me)^+$], 339 (5) [$(M-SiMe_3)^+$], 215 (18) [$(M-SiMePh_2)^+$], 98 (100) [$(H_2C{=}NC_5H_{10})^+$].

Synthesis of 14: The synthesis of **14** was analogous to that of *rac*-**8**. The residue was suspended in *n*-pentane (10 mL), freed from all salts, diluted with acetone (5 mL), and stored at −78 °C for 24 h. Thereafter, the formed nearly solid residue was separated from the solution at low temperature and the whole process was repeated twice more. Finally, all volatile compounds were removed in vacuo; yield: 420 mg, 0.45 mmol (75%). ^{1}H NMR (500.1 MHz, C_6D_6): $\delta = 0.28$, 0.29 (s, 9H each; $Si(CH_3)_3$), 0.40, 0.44 (AB system, $^2J_{AB} = 13.7$ Hz, 4H; $SiCH_2Ge$), 0.37 (s, 6H; $SiSiSiCH_3$), 0.96 (s, 6H; $CH_2Ge(CH_3)_2CH_2$), 1.35–1.45 (m, 4H; $NCCCH_2$), 1.55–1.65 (m, 8H; $NCCH_2C$), 2.40–2.50 (m, 8H; NCH_2CC), 2.426, 2.521 (AB system, $^2J_{AB} = 13.9$ Hz, 2H; $SiCH_2N$), 2.430, 2.523 (AB system, $^2J_{AB} = 13.9$ Hz, 2H; $SiCH_2N$), 7.30–7.40 (m, 12H; arom. H-*m*, H-*p*), 7.85–7.95 ppm (m, 8H; arom. H-*o*); {^{1}H}^{13}C NMR (125.8 MHz, C_6D_6): $\delta = -2.38$ (2C; $CH_2Ge(CH_3)_2CH_2$), −0.79 (2C; $SiCH_2Ge$), 0.20 (6C; $Si(CH_3)_3$), 3.66 (2C; $SiSiSiCH_3$), 24.2 (2C; $NCCCH_2$), 26.5 (4C; $NCCH_2C$), 49.4 (2C; $SiCH_2N$), 59.0 (4C; NCH_2CC), 128.08, 128.12 (4C each; C-*m*, C_6H_5Si), 128.99, 129.04 (2C each; C-*p*, C_6H_5Si), 135.64, 135.71 (4C each; C-*o*, C_6H_5Si), 138.44, 138.48 ppm (2C each, C-*i*, C_6H_5Si); {^{1}H}^{29}Si NMR (99.4 MHz, C_6D_6): $\delta = -41.8$ (2Si; $SiCH_2N$), −18.8 (2Si; $SiCH_3$), −15.9 ppm (2Si; $Si(CH_3)_3$); GC/EI-MS: $t_R = 13.61$ min [80 °C (2 min)–10 °C min^{-1}–280 °C (5 min)]; *m*/*z* (%): 924 (2) [M^+], 909 (4) [$(M-Me)^+$], 851 (11) [$(M-SiMe_3)^+$], 826 (3) [$(M-H_2C{=}NC_5H_{10})^+$], 728 (100) [$(M-(H_2C{=}NC_5H_{10})_2^+$], 514 (3) [{$(Ph_2MeSi)(SiMe_3)(CH_2NC_5H_{10})$]Si-[$CH_2Ge(CH_3)_2$]]$^+$, 498 (2) [{$(Ph_2MeSi)(SiMe_3)(CH_2NC_5H_{10})$]$Si(CH_2Ge{=}CH_2)^+$}, 197 (3) [$(Ph_2MeSi)^+$], 98 (100) [$(H_2C{=}NC_5H_{10})^+$]; elemental analysis (%) calcd for $C_{48}H_{78}NSi_6Ge$: C 62.4, H 8.51, N 3.03; found: C 61.7, H 8.48, N 3.63.

General conditions for the crystallization of the α-lithiated oligosilanes: A solution of the appropriate oligosilane (50 mg) in *n*-pentane [*V*(*n*-pentane)] was combined with a 1.7 M solution of *t*BuLi in *n*-pentane, which resulted in immediate cloudiness. The mixture was then stirred for 5 h at room temperature. After storing each solution at low temperature, the α-lithiated silanes could be successfully isolated as crystalline solids. Table 3 lists the full reaction conditions, crystallization temperatures, and quantities of the reactants used, as well as the solvents for the lithiation reactions.

Synthesis of (*R*,*R*)-16: (*R*,*R*)-TMCDA [(*R*,*R*)-**15**] (3.90 g, 22.9 mmol) was dissolved in *n*-pentane (20 mL) and the solution was cooled to −40 °C. At this temperature, a 1.7 M solution of *t*BuLi in *n*-pentane (17.6 mL, 29.9 mmol) was added, and the reaction mixture was allowed to slowly warm to room temperature and then stirred for a further 3 h. The mixture was then treated with dimethylphenylchlorosilane (5.12 g,

Table 3. Reactants, products, reaction conditions, and quantities for the lithiation reactions.

Reactant/*m*(reactant) [mg] (*n*-[mmol])	Product	Equiv. *t*BuLi (*n*-[mmol])	*V*(*n*-pentane) [mL]	Crystallization temperature [°C]
(*R*)-**3**/50 (0.17)	[*t*BuLi·(*R*)-**7**]$_2$	2 (0.34)	0.2	−78
rac-**3**/50 (0.17)	(*rac*-**7**)$_4$	1 (0.17)	0.2	−78
(*R*)-**6**/50 (0.15)	[*t*BuLi·(*R*)-**10**]$_2$	2 (0.30)	0.3	−78
rac-**4**/50 (0.12)	(*rac*-**12**)$_2$	1 (0.12)	0.3	−30

29.9 mmol) at −80 °C and the trapping reaction was allowed to proceed for 12 h at RT. The LiCl formed was dissolved by the addition of 2.5 M HCl (20 mL). After the addition of diethyl ether (10 mL), the combined organic layers were extracted with 2 M HCl (3×20 mL). The aqueous layers were subsequently adjusted to pH 12 with NaOH and extracted with diethyl ether (3×30 mL), and the combined organic layers were dried over Na_2SO_4. After removal of all volatile compounds in vacuo, the crude product was purified by bulb-to-bulb distillation (oven temperature: 160 °C, 2×10^{-2} mbar); yield: 4.32 g, 14.2 mmol (62 %). ^{1}H NMR (500.1 MHz, C_6D_6): δ = 0.50 (s, 3H; $Si(CH_3)$), 0.51 (s, 3H; $Si(CH_3)$), 1.03–1.17 (m, 4H; 2CH_2, cyclohexyl), 1.70–1.73 (m, 2H; CH_2, cyclohexyl), 1.84–1.89 (m, 2H; CH_2, cyclohexyl), 2.26 (AB system, $^2J_{AB}$ = 14.2 Hz, 1H; $N(CH_2)Si$, D1), 2.35 (s, 3H; $N(CH_3)CH_2Si$), 2.38 (s, 6H; $N(CH_3)_2$), 2.36–2.43 (m, 2H; CHN), 2.53 (AB system, $^2J_{AB}$ = 14.2 Hz, 1H; $N(CH_2)Si$, D2), 7.34–7.36 (m, 3H; arom. H), 7.75–7.77 ppm (m, 2H; arom. H); {^{1}H}^{13}C NMR (125.8 MHz, C_6D_6): δ = −2.43, −2.40 ($Si(CH_3)_2$), 24.8 (CH_2CHN), 25.0 (CH_2CHN), 26.1 (($CH_2)_2CH_2$), 40.4 ($N(CH_3)CH_2Si$), 40.5 ($N(CH_3)_2$), 44.2 ($N(CH_2)Si$), 64.3 (CHN), 67.1 (CHN), 128.0 (C-*m*, C_6H_5), 129.1 (C-*p*, C_6H_5), 134.2 (C-*o*, C_6H_5), 139.9 ppm (C-*i*, C_6H_5); ^{29}Si NMR (99.4 MHz, C_6D_6): δ = −6.2; $[\alpha]_D^{20}$ = −15.1 (cyclohexane, 0.7784 g/100 mL); GC/EI-MS: t_R = 9.71 min [80 °C (2 min)–10 °C min^{-1}–280 °C (5 min)]; *m*/*z* (%): 304 (6) [*M*$^+$], 218 (25) [{*M*−$CH_2CH_2CH_2N(CH_3)_2$}$^+$], 169 (85) [{*M*−$Si(CH_3)_2Ph$}$^+$], 135 (50) [{$Si(CH_3)_2Ph$}$^+$], 124 (95) [{$C_6H_9N(CH_3)CH_2$}$^+$], 58 (100) [{$N(CH_3)_2CH_2$}$^+$]; elemental analysis (%) calcd for $C_{18}H_{32}N_2Si$: C 71.0, H 10.7, N 9.2; found: C 71.0, H 10.6, N 9.2.

Crystallization of the α-lithiated silane 17: Silane (*R*,*R*)-**16** (120 mg, 0.39 mmol) was dissolved in pentane (0.8 mL) and the solution was cooled to −100 °C. At this temperature, a 1.5 M solution of *t*BuLi in pentane/hexane (0.3 mL, 0.45 mmol) was added and the mixture was slowly warmed to −78 °C. Storage at −78 °C for 24 h gave colorless crystals of the diastereomerically pure compound (*R*,*R*,S_{Si})-**17**. Addition of the alkyllithium at −40 °C and subsequent cooling to −78 °C yielded crystals of the 1:1 aggregate of the respective diastereomers (*R*,*R*,S_{Si})-**17** and (*R*,*R*,R_{Si})-**17**.

Trapping of 17 to form (*R*,*R*)-18: (*R*,*R*)-**16** (500 mg, 1.64 mmol) was dissolved in *n*-pentane (5 mL) and the solution was cooled to −110 °C. At this temperature, a 1.2 M solution of *t*BuLi in pentane (1.4 mL, 1.68 mmol) was added and the reaction mixture was slowly warmed to −78 °C. After storage at this temperature for 24 h, the intermediate was trapped with trimethyltin chloride (380 mg, 1.91 mmol) and the mixture was stirred for an additional 16 h at room temperature. Work-up was accomplished in the same manner as for compound **16**, extracting with aqueous acid, making the combined aqueous extracts alkaline, and extracting the aqueous phase with diethyl ether. After removal of all volatile compounds from the combined extracts in vacuo, the crude product was purified by bulb-to-bulb distillation to afford **18** as a 79:21 mixture of the two diastereomers as a colorless oil (oven temperature: 235 °C, 5×10^{-3} mbar). Yield: 523 mg, 1.12 mmol (68 %). Major isomer: ^{1}H NMR (500.1 MHz, C_6D_6): δ = 0.19 (s, $^2J_{H,^{117}Sn}$ = 25.6 Hz, $^2J_{H,^{119}Sn}$ = 26.8 Hz, 9H; $SnCH_3$), 0.33 (s, $^2J_{H,^{117}Sn}$ = 24.9 Hz, $^2J_{H,^{119}Sn}$ = 26.1 Hz, 2H; $SnCH_2Si$), 0.59 (s, 3H; $SiCH_3$), 1.05–1.10 (m, 4H; 2CH_2, cyclohexyl), 1.71–1.75 (m, 2H; CH_2, cyclohexyl), 1.83–1.86 (m, 1H; CH_2, cyclohexyl), 1.93–1.97 (m, 1H; CH_2, cyclohexyl), 2.38, 2.60 (AB system, $^2J_{AB}$ = 14.0 Hz, 2H; $N(CH_2)Si$), 2.37 (s, 3H; $N(CH_3)CH_2Si$), 2.39 (s, 6H; $N(CH_3)_2$), 2.39–2.43 (m, 2H; CHN), 7.28–7.39 (m, 3H; arom. H), 7.74–7.79 ppm (m, 2H; arom. H); {^{1}H}^{13}C NMR (125.8 MHz, C_6D_6): δ = −7.95 ($^1J_{^{13}C,^{117}Sn}$ = 158.7 Hz, $^1J_{^{13}C,^{119}Sn}$ = 166.3 Hz; $SnCH_3$), −6.80 ($SiCH_2Sn$), −1.64 ($SiCH_3$), 24.7 + 25.2 + 26.1 + 26.2 (CH_2, cyclohexyl), 40.5 ($N(CH_3)_2$), 40.6 (NCH_3), 45.68 (NCH_2Si), 64.4 (CHN), 67.0 (CHN), 127.9 (C-*m*, C_6H_5), 129.0 (C-*p*, C_6H_5), 134.2 (C-*o*, C_6H_5), 140.8 ppm (C-*i*, C_6H_5); ^{29}Si NMR (99.4 MHz, C_6D_6): δ = −3.86 ppm; ^{119}Sn NMR (186.5 MHz, C_6D_6): δ = 6.54 ppm; GC/EI-MS: t_R = 10.92 min [80 °C (2 min)–10 °C min^{-1}–280 °C (5 min)]; *m*/*z* (%): 468 (1) [*M*$^+$], 453 (3) [{*M*−CH_3}$^+$], 169 (100) [{*M*−$PhSi(CH_3)CH_2SnMe_3$}$^+$], 135 (25) [{$Si(CH_3)_2Ph$}$^+$], 124 (78) [{$C_6H_9N(CH_3)CH_2$}$^+$], 58 (82) [{$N(CH_3)_2CH_2$}$^+$]. Minor isomer: ^{1}H NMR (500.1 MHz, C_6D_6): δ = 0.19 (s, $^2J_{H,^{117}Sn}$ = 25.6 Hz, $^2J_{H,^{119}Sn}$ = 26.7 Hz, 9H; $SnCH_3$), 0.34 (s, $^2J_{H,^{117}Sn}$ = 24.8 Hz, $^2J_{H,^{119}Sn}$ = 26.0 Hz, 2H; $SnCH_2Si$), 0.60 (s, 3H; $Si(CH_3)$), 1.06–1.11 (m, 4H; 2CH_2, cyclohexyl), 1.72–1.76 (m, 2H; CH_2, cyclohexyl), 1.83–1.86 (m, 1H; CH_2, cyclohexyl), 1.93–1.97 (m, 1H; CH_2, cyclohexyl), 2.36, 2.55 (AB system, $^2J_{AB}$ = 14.2 Hz, 1H; $N(CH_2)Si$), 2.37 (s, 3H; $N(CH_3)CH_2Si$), 2.39 (s, 6H; $N(CH_3)_2$), 2.38–2.43 (m, 2H; CHN), 7.29–7.38 (m, 3H; arom. H), 7.73–7.79 ppm (m, 2H; arom. H); {^{1}H}^{13}C NMR (125.8 MHz, C_6D_6): δ = −7.92 ($^1J_{^{13}C,^{117}Sn}$ = 158.8 Hz, $^1J_{^{13}C,^{119}Sn}$ = 166.4 Hz; $SiCH_3$), −6.84 ($SiCH_2Sn$), −1.79 ($SiCH_3$), 24.7 + 25.2 + 26.1 + 26.6 (CH_2, cyclohexyl), 40.7 ($N(CH_3)_2$), 40.9 (NCH_3), 45.70 (NCH_2Si), 64.5 (CHN), 66.9 (CHN), 128.0 (C-*m*, C_6H_5), 129.1 (C-*p*, C_6H_5), 134.1 (C-*o*, C_6H_5), 140.9 ppm (C-*i*, C_6H_5); ^{29}Si NMR (99.4 MHz, C_6D_6): δ = −3.87 ppm; ^{119}Sn NMR (186.5 MHz, C_6D_6): δ = −6.33 ppm; GC/EI-MS: as for major isomer.

General procedure for the trapping reaction of 17 with tributyltin chloride: Silane (*R*,*R*)-**16** (120 mg, 0.39 mmol) was dissolved in pentane (0.8 mL) and the solution was cooled to the first temperature indicated in Table 1. At this temperature, a 1.5 M solution of *t*BuLi in pentane (0.3 mL, 0.45 mmol) was added and the mixture was slowly allowed to warm over a period of 24 h to the second temperature indicated in Table 1. After trapping of the intermediate with tributyltin chloride (280 mg, 0.85 mmol) and addition of diethyl ether (10 mL), the mixture was acidified to pH 1 and the organic phase was extracted three times with water. The combined aqueous phases were then made alkaline to pH 12, extracted with diethyl ether (5×30 mL), and the combined organic layers were dried over Na_2SO_4. After removal of all volatile compounds in vacuo, the crude product was examined by NMR spectrometry. Major diastereomer: ^{1}H NMR (500.1 MHz, C_6D_6): δ = 0.22 (s, $^2J_{1\text{-}H,^{117}Sn}$ = 31.1 Hz, $^2J_{1\text{-}H,^{119}Sn}$ = 32.2 Hz, 2H; $SiCH_2Sn$), 0.63 (s, $^4J_{1\text{-}H,^{117/119}Sn}$ = 20.0 Hz, 3H; $SiCH_3$), 0.98 (t, ^3J = 7.33 Hz, 6H; $SnCH_2$), 1.03 (t, ^3J = 7.27 Hz, 9H; $SnCH_2CH_2CH_2CH_3$), 0.98–1.10 (m, 4H; 2CH_2, cyclohexyl), 1.44–1.48 (m, 6H; $SnCH_2CH_2CH_2$), 1.57–1.63 (m, 6H; $SnCH_2CH_2$), 1.81–1.87 (m, 2H; CH_2, cyclohexyl), 1.93–1.97 (m, 2H; CH_2, cyclohexyl), 2.35, 2.62 (AB system, $^2J_{AB}$ = 14.0 Hz, 2H; $N(CH_2)Si$), 2.36 (s, 3H; $N(CH_3)CH_2Si$), 2.40 (s, 6H; $N(CH_3)_2$), 2.39–2.43 (m, 2H; CHN), 7.29–7.38 (m, 3H; arom. H), 7.71–7.80 ppm (m, 2H; arom. H); {^{1}H}^{13}C NMR (125.8 MHz, C_6D_6): δ = −9.59 ($^1J_{^{13}C,^{117}Sn}$ = 93.9 Hz, $^1J_{^{13}C,^{119}Sn}$ = 98.1 Hz; $SiCH_2Sn$), −1.49 ($^1J_{^{13}C,^{29}Si}$ = 3.77 Hz; $SiCH_3$), 10.7 ($^1J_{^{13}C,^{117}Sn}$ = 155.3 Hz, $^1J_{^{13}C,^{119}Sn}$ = 162.6 Hz; $SnCH_2$), 13.9 ($^4J_{^{13}C,^{117/119}Sn}$ = 3.9 Hz; $SnCH_2CH_2CH_2CH_3$), 24.9 + 25.2 + 26.1 + 26.2 (CH_2, cyclohexyl), 27.8 ($^3J_{^{13}C,^{117}Sn}$ = 28.34 Hz, $^3J_{^{13}C,^{119}Sn}$ = 29.64 Hz; $SnCH_2CH_2CH_2$), 29.6 ($^2J_{^{13}C,^{117/119}Sn}$ = 9.70 Hz; $SnCH_2CH_2$), 40.5 ($N(CH_3)_2$), 40.7 (NCH_3), 46.0 (NCH_2Si), 64.49 (CHN), 67.1 (CHN), 127.9 (C-*m*, C_6H_5), 128.9 (C-*p*, C_6H_5), 134.20 (C-*o*, C_6H_5), 141.0 ppm (C-*i*, C_6H_5); ^{29}Si NMR (99.4 MHz, C_6D_6): δ = −3.6 ppm ($^2J_{^{29}Si,^{117/119}Sn}$ = 11.5 Hz); ^{119}Sn NMR (186.5 MHz, C_6D_6): δ = −0.7 ppm. Minor diastereomer: ^{1}H NMR (500.1 MHz, C_6D_6): δ = 0.24 (s, $^2J_{1\text{-}H,^{117}Sn}$ = 31.1 Hz, $^2J_{1\text{-}H,^{119}Sn}$ = 32.2 Hz, 2H; $SiCH_2Sn$), 0.64 (s, 3H; $SiCH_3$), 0.98 (t, $^3J_{HH}$ = 7.33 Hz, 6H; $SnCH_2$), 1.03 (t, $^3J_{HH}$ = 7.27 Hz, 9H; $SnCH_2CH_2CH_2CH_3$), 0.98–1.10 (m, 4H; 2CH_2, cyclohexyl), 1.44–1.48 (m, 6H; $SnCH_2CH_2CH_2$), 1.57–1.63 (m, 6H; $SnCH_2CH_2$), 1.84–1.87 (m, 2H; CH_2, cyclohexyl), 1.93–1.97 (m, 2H; CH_2, cyclohexyl), 2.26, 2.55 (AB system, $^2J_{AB}$ = 14.0 Hz, 2H; $N(CH_2)Si$), 2.35 (s, 3H; $N(CH_3)CH_2Si$), 2.38 (s, 6H; $N(CH_3)_2$), 2.39–2.43 (m, 2H; CHN), 7.29–7.38 (m, 3H; arom. H), 7.71–7.80 ppm (m, 2H; arom. H); {^{1}H}^{13}C NMR (125.8 MHz, C_6D_6): δ = −9.66 ($^1J_{^{13}C,^{119}Sn}$ = 98.1 Hz, $^1J_{^{13}C,^{117}Sn}$ =

93.9 Hz; $SiCH_2Sn$), −1.56 ($SiCH_3$), 8.3 ($^1J_{^{13}C,^{117}Sn}$ = 155.3 Hz, $^1J_{^{13}C,^{117}Sn}$ = 162.6 Hz; $SnCH_2$), 14.1 ($^4J_{^{13}C,^{117/119}Sn}$ = 3.9 Hz, $SnCH_2CH_2CH_2CH_3$), 24.7 + 25.2 + 26.1 + 26.6 (CH_2, cyclohexyl), 27.8 ($^3J_{^{13}C,^{117}Sn}$ = 28.34 Hz, $^3J_{^{13}C,^{119}Sn}$ = 29.64 Hz; $SnCH_2CH_2CH_2$), 29.8 ($^2J_{^{13}C,^{117/119}Sn}$ = 9.70 Hz; $SnCH_2CH_2$), 40.5 ($N(CH_3)_2$), 40.8 (NCH_3), 45.9 ($N(CH_2)Si$), 64.54 (CHN), 67.0 (CHN), 128.0 (C-*m* or C-*o*, C_6H_5), 129.0 (C-*p*, C_6H_5), 134.16 (C-*m* or C-*o*, C_6H_5), 141.1 ppm (C-*i*, C_6H_5); ^{29}Si NMR (99.4 MHz, C_6D_6): $\delta = -3.6$ ppm ($^2J_{^{29}Si,^{117/119}Sn}$ = 11.5 Hz); ^{119}Sn NMR (186.5 MHz, C_6D_6): $\delta = -0.9$ ppm.

Crystallographic details: Crystallographic data for (*R*)-**7**, (*R*)-**10**, *rac*-**12**, (*R*,*R*,S_{Si})-**17**, and the 1:1 aggregate of **17** were collected with a Bruker APEX-CCD (D8 three-circle goniometer) (Bruker AXS). Cell determination and refinement were carried out with Smart version 5.622 (Bruker AXS, 2001), integration with SaintPlus version 6.02 (Bruker AXS, 1999), and empirical absorption correction with SADABS version 2.01 (Bruker AXS, 1999). Crystallographic data for *rac*-**7** were collected with a Stoe-IPDS diffractometer. Cell determination was carried out with Cell (Stoe & Cie, 1997), cell refinement with Integrate (Stoe & Cie, 1999), and numerical absorption correction with Faceit (Stoe & Cie, 1997). Crystals of each of the compounds were mounted in an inert oil (perfluoropolyalkyl ether) at −60 °C (N_2 stream) using the X-TEMP 2 device (T. Kottke, D. Stalke, *J. Appl. Crystallogr.* **1993**, *26*, 615; T. Kottke, R. J. Lagow, D. Stalke, *J. Appl. Crystallogr.* **1996**, *29*, 615; D. Stalke, *Chem. Soc. Rev.* **1998**, *27*, 171). The crystal structure determinations were carried out at −100 °C ($Mo_{K\alpha}$ radiation, λ = 0.71073 Å). The structures were solved by direct and Fourier methods using SHELXS-90 (G. M. Sheldrick, University of Göttingen, 1990) and SHELXL-97 (G. M. Sheldrick, SHELXL97, University of Göttingen, 1997). CCDC-745695 (*rac*-**7**), 745696 [(*R*)-**7**], 745697 [(*R*)-**10**], 745698 (*rac*-**12**), 745699 [(*R*,*R*,S_{Si})-**17**], and 745700 (1:1 aggregate of **17**) contain the detailed crystallographic data. Copies of the data can be obtained free of charge via www.ccdc.cam.ac.uk/data_request/cif or on application to the Cambridge Crystallographic Data Centre, 12 Union Road, Cambridge CB2 1EZ, UK; fax: (+44) 1223-336033; email: deposit@ccdc.cam.ac.uk. Further information is available in the Supporting Information.

Computational details: All calculations were performed without symmetry restrictions. Starting coordinates were obtained with Chem3DUltra 10.0. Optimization and additional harmonic vibrational frequency analyses (to establish the nature of stationary points on the potential energy surface) were performed with the software package Gaussian 03 (Revision D.01 and Revision E.01) at the same level.[31] The total (SCF) and zero-point energies (ZPE), all reaction barriers, and the coordinates of all systems are available in the Supporting Information. Global minima and vibrational frequency analyses were performed at the B3LYP/6-31+G(d) and/or M052X/6-31+G(d) level. The vibrational frequency analyses showed imaginary frequencies for the transition states representing the corresponding vibration for the deprotonation. For the educts, no imaginary frequencies were obtained. For polar compounds, entropy is crucially influenced by solvent effects. Additionally calculated Gibbs free energies seem to be less reliable in such large systems due to very low frequencies, at which the harmonic oscillator model produces significant deviations.[32] Thus, only enthalpy values are discussed. Corrections for basis set superposition errors (BSSE) have not been applied.

Acknowledgements

We are grateful to the Deutsche Forschungsgemeinschaft and the Fonds der Chemischen Industrie for financial support and the award of a doctoral scholarship (to V.H.G.). C.D. thanks the Studienstiftung des deutschen Volkes for a doctoral scholarship. We gratefully acknowledge Chemetall GmbH and Wacker Chemie AG for providing us with specialty chemicals.

[1] For selected applications, see: a) H.-S. Oh, L.-S. Park, Y. Kawakami, *Chirality* **2003**, *15*, 646; b) W. Uhlig, *J. Organomet. Chem.* **2003**, *685*, 70; c) K. Tamao, A. Kawachi, *Adv. Organomet. Chem.* **1995**, *38*, 1; d) P. D. Lickiss, C. M. Smith, *Coord. Chem. Rev.* **1995**, *145*, 75; e) A. Sekiguchi, V. Y. Lee, M. Nanjo, *Coord. Chem. Rev.* **2000**, *210*, 11.

[2] For example, see: a) B. H. Lipshutz, N. Tanaka, B. R. Taft, C.-T. Lee, *Org. Lett.* **2006**, *8*, 1963; b) B. Zhu, J. S. Panek, *Eur. J. Org. Chem.* **2001**, 1701; c) M. Oestreich, *Synlett* **2007**, 1629.

[3] For example, see: a) S. Rendler, M. Oestreich, C. P. Butts, G. C. Lloyd-Jones, *J. Am. Chem. Soc.* **2007**, *129*, 502; b) P. J. Stang, A. E. Learned, *J. Org. Chem.* **1989**, *54*, 1779.

[4] G. T. Notte, J. L. Leighton, *J. Am. Chem. Soc.* **2008**, *130*, 6676.

[5] S. Shirakawa, P. J. Lombardi, J. L. Leighton, *J. Am. Chem. Soc.* **2005**, *127*, 9974.

[6] S. Shirakawa, R. Berger, J. L. Leighton, *J. Am. Chem. Soc.* **2005**, *127*, 2858.

[7] a) S. E. Denmark, T. Wynn, G. L. Beutner, *J. Am. Chem. Soc.* **2002**, *124*, 13405; b) S. E. Denmark, G. L. Beutner, *J. Am. Chem. Soc.* **2003**, *125*, 7800.

[8] S. Rendler, G. Auer, M. Oestreich, *Angew. Chem.* **2005**, *117*, 7793; *Angew. Chem. Int. Ed.* **2005**, *44*, 7620.

[9] For one example, see: M. Trzoss, J. Shao, S. Bienz, *Tetrahedron: Asymmetry* **2004**, *15*, 1501.

[10] For one example, see: M. Oestreich, U. K. Schmid, G. Auer, M. Keller, *Synthesis* **2003**, 2725.

[11] C. Strohmann, J. Hörnig, D. Auer, *J. Chem. Soc. Chem. Commun.* **2002**, 766.

[12] For example, see: a) C. Strohmann, C. Däschlein, M. Kellert, D. Auer, *Angew. Chem.* **2007**, *119*, 4864; *Angew. Chem. Int. Ed.* **2007**, *46*, 4780; b) C. Strohmann, C. Däschlein, *Organometallics* **2008**, *27*, 2499; c) C. Däschlein, V. H. Gessner, C. Strohmann, *Acta Crystallogr. Sect. E* **2008**, *64*, o1950; d) L. H. Sommer, R. Mason, *J. Am. Chem. Soc.* **1965**, *87*, 1619; e) L. H. Sommer, J. E. Lyons, H. Fujimoto, *J. Am. Chem. Soc.* **1969**, *91*, 7051; f) E. Colomer, R. J. P. Corriu, *J. Chem. Soc. Chem. Commun.* **1976**, 176; g) E. Colomer, R. J. P. Corriu, *J. Organomet. Chem.* **1977**, *133*, 159.

[13] For selected examples of studies on lithiosilanes, see: C. Strohmann, C. Däschlein, D. Auer, *J. Am. Chem. Soc.* **2006**, *128*, 704; b) C. Strohmann, C. Däschlein, *Chem. Commun.* **2008**, 2791; c) C. Däschlein, C. Strohmann, *Eur. J. Inorg. Chem.* **2009**, 43; d) C. Strohmann, O. Ulbrich, D. Auer, *Eur. J. Inorg. Chem.* **2001**, 1013; e) H.-W. Lerner, S. Scholz, M. Bolte, M. Wagner, *Z. Anorg. Allg. Chem.* **2004**, *630*, 443; f) T. I. Kückmann, F. Dornhaus, M. Bolte, H.-W. Lerner, M. C. Holthausen, M. Wagner, *Eur. J. Inorg. Chem.* **2007**, 1989; g) H.-W. Lerner, *Coord. Chem. Rev.* **2005**, *249*, 781; h) M. Omote, T. Tokita, Y. Shimizu, I. Imae, E. Shirakawa, Y. Kawakami, *J. Organomet. Chem.* **2000**, *611*, 20; i) D. Bravo-Zhivotovskii, I. Ruderfer, S. Melamed, M. Botoshansky, B. Tumanskii, Y. Apeloig, *Angew. Chem.* **2005**, *117*, 749; *Angew. Chem. Int. Ed.* **2005**, *44*, 739; j) C. Strohmann, M. Bindl, V. C. Vraaß, J. Hörnig, *Angew. Chem.* **2004**, *116*, 1029; *Angew. Chem. Int. Ed.* **2004**, *43*, 1011; k) D. Scheschkewitz, *Angew. Chem.* **2004**, *116*, 3025; *Angew. Chem. Int. Ed.* **2004**, *43*, 2965; l) M. Oestreich, G. Auer, M. Keller, *Eur. J. Org. Chem.* **2005**, 184; m) C. Däschlein, C. Strohmann, *Dalton Trans.* **2010**, DOI: 10.1039/b920846a.

[14] For studies on silyl anions, see: a) J. B. Lambert, M. Urdaneta-Perez, H.-N. Sun, *J. Chem. Soc. Chem. Commun.* **1976**, 806; b) J. B. Lambert, M. Urdaneta-Perez, *J. Am. Chem. Soc.* **1978**, *100*, 157; c) M. Flock, C. Marschner, *Chem. Eur. J.* **2002**, *8*, 1024; d) M. Flock, C. Marschner, *Chem. Eur. J.* **2005**, *11*, 4635.

[15] D. R. Schmidt, S. J. O'Malley, J. L. Leighton, *J. Am. Chem. Soc.* **2003**, *125*, 1190.

[16] For one example concerning the reactivity of alkyllithium compounds towards disilanes, see: W. C. Still, *J. Org. Chem.* **1976**, *41*, 3063.

[17] For selected examples, see: a) T. H. Chan, P. J. Pellon, *J. Am. Chem. Soc.* **1989**, *111*, 8737; b) T. H. Chan, S. Lamonthe, *Tetrahedron Lett.* **1991**, *32*, 1847; c) T. H. Chan, K. T. Nwe, *J. Org. Chem.* **1992**, *57*, 6107; d) C. Strohmann, B. C. Abele, K. Lehmen, F. Villafane, L. Sierra, S. Martín-Barrios, D. Schildbach, *J. Organomet. Chem.* **2002**, *661*, 149; e) C. Strohmann, B. C. Abele, K. Lehmen, D. Schildbach, *Angew. Chem.* **2005**, *117*, 3196; *Angew. Chem. Int. Ed.* **2005**, *44*,

3136; f) C. Strohmann, K. Lehmen, S. Dilsky, *J. Am. Chem. Soc.* **2006**, *128*, 8102; g) C. Däschlein, J. O. Bauer, C. Strohmann, *Angew. Chem.* **2009**, *121*, 8218–8221; *Angew. Chem. Int. Ed.* **2009**, *48*, 8074–8077; lit h > C. Däschlein, C. Strohmann, *Z. Naturforsch.* **2009**, *64b*, 1558–1566

[18] Review concerning side-arm complexation: G. W. Klumpp, *Recl. Trav. Chim. Pays-Bas* **1986**, *105*, 1.

[19] For selected examples, see: a) C. Strohmann, K. Lehmen, K. Wild, D. Schildbach, *Organometallics* **2002**, *21*, 3079; b) C. Strohmann, D. H. M. Buchhold, T. Seibel, K. Wild, D. Schildbach, *Eur. J. Inorg. Chem.* **2003**, 3453; c) H. Ott, C. Däschlein, D. Leusser, D. Schildbach, T. Seibel, D. Stalke, C. Strohmann, *J. Am. Chem. Soc.* **2008**, *130*, 11901.

[20] The enantiomeric ratio of (*R*)-**8** was determined by treatment of the functionalized disilane with three equivalents of (*R*)-mandelic acid in $CDCl_3$. This resulted in the formation of a diastereomeric salt, the ^{1}H NMR resonance signals of the trimethylstannyl group in which could be integrated separately. Comparison of the spectra of the racemic and enantiomerically pure compounds gave an e.r. of >99:1 as no signal due to the second possible diastereomer was detected.

[21] The enantiomeric ratio of (*R*)-**9** was determined by treatment of the functionalized disilane with an excess of tris[3-(heptafluoropropylhydroxymethylene)-(+)-camphorato]europium(III) in $CDCl_3$. This resulted in separation of the resonance signals of the $SiMe_3$ group in the ^{1}H NMR spectrum. Comparison of the spectra of the racemic and enantiomerically pure compounds gave an e.r. of >99:1 as no signal due to the second possible diastereomer was detected.

[22] a) V. H. Gessner, C. Däschlein, C. Strohmann, *Chem. Eur. J.* **2009**, *15*, 3320; b) T. Stey, D. Stalke, in *The Chemistry of Organolithium Compounds* (Eds.: Z. Rappoport, I. Marek), Wiley, New York, **2004**, pp. 47–120.

[23] For examples of mixed aggregates, see: a) C. M. P. Kronenburg, E. Rijnberg, J. T. B. H. Jastrzebski, H. Kooijman, M. Lutz, A. L. Spek, R. A. Gossage, G. van Koten, *Chem. Eur. J.* **2005**, *11*, 253; b) R. A. Gossage, J. T. B. H. Jastrzebski, G. van Koten, *Angew. Chem.* **2005**, *117*, 1472; *Angew. Chem. Int. Ed.* **2005**, *44*, 1448; c) P. A. Chase, M. Lutz, A. L. Spek, R. A. Gossage, G. van Koten, *Dalton Trans.* **2008**, 5783; d) D. Bravo-Zhivotovskii, G. Molev, V. Kravchenko, M. Botoshansky, A. Schmidt, Y. Apeloig, *Organometallics* **2006**, *25*, 4719; e) B. Goldfuss, M. Steigelmann, F. Rominger, H. Urtel, *Chem. Eur. J.* **2001**, *7*, 4456; f) B. Goldfuss, M. Steigelmann, F. Rominger, *Angew. Chem.* **2000**, *112*, 4299; *Angew. Chem. Int. Ed.* **2000**, *39*, 4133; g) B. Goldfuss, S. I. Khan, K. N. Houk, *Organometallics* **1999**, *18*, 2927; h) J. Arnold, V. Knapp, J. A. R. Schmidt, A. Shafir, *Dalton Trans.* **2002**, 3273.

[24] For some examples of organolithium structures, see: a) R. E. Mulvey, *Chem. Soc. Rev.* **1998**, *27*, 339; b) W. N. Setzer, P. v. R. Schleyer, *Adv. Organomet. Chem.* **1985**, *24*, 353; c) E. Weiss, *Angew. Chem.* **1993**, *105*, 1565; *Angew. Chem. Int. Ed. Engl.* **1993**, *32*, 1501; d) C. Strohmann, K. Strohfeldt, D. Schildbach, M. J. McGrath, P. O'Brien, *Organometallics* **2004**, *23*, 5389; e) T. Kottke, D. Stalke, *Angew. Chem.* **1993**, *105*, 619; *Angew. Chem. Int. Ed. Engl.* **1993**, *32*, 580; f) T. Kottke, D. Stalke, *Angew. Chem.* **1993**, *105*, 619; *Angew. Chem. Int. Ed. Engl.* **1993**, *32*, 580; g) U. Siemeling, T. Redecker, B. Neumann, H.-G. Stammler, *J. Am. Chem. Soc.* **1994**, *116*, 5507; h) C. Strohmann, K. Strohfeldt, D. Schildbach, *J. Am. Chem. Soc.* **2003**, *125*, 13672; i) C. Strohmann, V. H. Gessner, *Z. Anorg. Allg. Chem.* **2007**, *633*, 2285; j) C. Strohmann, V. H. Gessner, A. Damme, *Chem. Commun.* **2008**, 3381; k) V. H. Gessner, C. Strohmann, *J. Am. Chem. Soc.* **2008**, *130*, 14412; l) C. Strohmann, V. H. Gessner, *Chem. Asian J.* **2008**, *3*, 1929; m) E. A. C. Lucken, E. Weiss, *J. Organomet. Chem.* **1964**, *2*, 197; n) E. Weiss, T. Lambertsen, B. Schubert, J. K. Cockcroft, A. Wiedenmann, *Chem. Ber.* **1990**, *123*, 79.

[25] a) C. M. Whisler, S. MacNeil, V. Snieckus, P. Beak, *Angew. Chem.* **2004**, *116*, 2256; *Angew. Chem. Int. Ed.* **2004**, *43*, 2206; b) C. G. Hartung, V. Snieckus, in *Modern Arene Chemistry* (Ed.: D. Astruc), Wiley-VCH, Weinheim, **2002**, pp. 330–367; c) P. Beak, A. I. Meyers, *Acc. Chem. Res.* **1986**, *19*, 356.

[26] A. D. Becke, *J. Chem. Phys.* **1993**, *98*, 5648.

[27] a) C. Strohmann, V. H. Gessner, *Angew. Chem.* **2007**, *119*, 8429; *Angew. Chem. Int. Ed.* **2007**, *46*, 8281; b) C. Strohmann, V. H. Gessner, *J. Am. Chem. Soc.* **2007**, *129*, 8952; c) C. Strohmann, V. H. Gessner, *J. Am. Chem. Soc.* **2008**, *130*, 11719.

[28] For further examples of lithiated tertiary methylamines, see: a) F. H. Köhler, N. Hertkorn, J. Blümel, *Chem. Ber.* **1987**, *120*, 2081; b) S. Harder, M. Lutz, *Organometallics* **1994**, *13*, 5173; c) M. Schakel, M. P. Aarnts, G. W. Klumpp, *Recl. Trav. Chim. Pays-Bas* **1990**, *109*, 305; d) G. W. Klumpp, H. Luitjes, M. Schakel, E. J. J. de Kanter, R. F. Schmitz, N. J. R. van Eikema Hommes, *Angew. Chem.* **1992**, *104*, 624; *Angew. Chem. Int. Ed. Engl.* **1992**, *31*, 633; e) C. Strohmann, V. H. Gessner, *Angew. Chem.* **2007**, *119*, 4650; *Angew. Chem. Int. Ed.* **2007**, *46*, 4566; f) H. H. Karsch, *Chem. Ber.* **1996**, *129*, 483; g) D. Bojer, I. Kamps, X. Tian, A. Hepp, T. Pape, R. Fröhlich, N. W. Mitzel, *Angew. Chem.* **2007**, *119*, 4254; *Angew. Chem. Int. Ed.* **2007**, *46*, 4176.

[29] a) S. E. Denmark, N. Nakajima, O. J.-C. Nicaise, *J. Am. Chem. Soc.* **1994**, *116*, 8797; b) C. A. Gittins née Jones, M. North, *Tetrahedron: Asymmetry* **1997**, *8*, 3789; c) S. Arrasate, E. Lete, N. Sotomayor, *Tetrahedron: Asymmetry* **2001**, *12*, 2077; d) D. A. Pflum, D. Krishnamurthy, Z. Han, S. A. Wald, C. H. Senanayake, *Tetrahedron Lett.* **2002**, *43*, 923; e) M. J. McGrath, J. L. Bilke, P. O'Brien, *Chem. Commun.* **2006**, 2607.

[30] J. F. Larrow, E. N. Jacobsen, *J. Org. Chem.* **1994**, *59*, 1939; b) J.-C. Kizirian, N. Cabello, L. Pinchard, J.-C. Caille, A. Alexakis, *Tetrahedron* **2005**, *61*, 8939; d) C. Strohmann, V. H. Gessner, *J. Am. Chem. Soc.* **2008**, *130*, 11719.

[31] Gaussian 03 (Revision D.01, Revision E.01), M. J. Frisch, G. W. Trucks, H. B. Schlegel, G. E. Scuseria, M. A. Robb, J. R. Cheeseman, J. A. Montgomery, Jr., T. Vreven, K. N. Kudin, J. C. Burant, J. M. Millam, S. S. Iyengar, J. Tomasi, V. Barone, B. Mennucci, M. Cossi, G. Scalmani, N. Rega, G. A. Petersson, H. Nakatsuji, M. Hada, M. Ehara, K. Toyota, R. Fukuda, J. Hasegawa, M. Ishida, T. Nakajima, Y. Honda, O. Kitao, H. Nakai, M. Klene, X. Li, J. E. Knox, H. P. Hratchian, J. B. Cross, V. Bakken, C. Adamo, J. Jaramillo, R. Gomperts, R. E. Stratmann, O. Yazyev, A. J. Austin, R. Cammi, C. Pomelli, J. W. Ochterski, P. Y. Ayala, K. Morokuma, G. A. Voth, P. Salvador, J. J. Dannenberg, V. G. Zakrzewski, S. Dapprich, A. D. Daniels, M. C. Strain, O. Farkas, D. K. Malick, A. D. Rabuck, K. Raghavachari, J. B. Foresman, J. V. Ortiz, Q. Cui, A. G. Baboul, S. Clifford, J. Cioslowski, B. B. Stefanov, G. Liu, A. Liashenko, P. Piskorz, I. Komaromi, R. L. Martin, D. J. Fox, T. Keith, M. A. Al-Laham, C. Y. Peng, A. Nanayakkara, M. Challacombe, P. M. W. Gill, B. Johnson, W. Chen, M. W. Wong, C. Gonzalez, J. A. Pople, Gaussian, Inc., Wallingford CT, **2004**.

[32] E.-U. Würthwein, D. Hoppe, *J. Org. Chem.* **2005**, *70*, 4443.

Received: September 16, 2009
Published online: February 24, 2010

